1 # A Non-Canonical Function of Arabidopsis ERECTA
2 # Proteins in Gibberellin Signaling

3

4 Elzbieta Sarnowska[a#], Szymon Kubala[b#], Pawel Cwiek[b#], Sebastian Sacharowski[b], Paulina
5 Oksinska[b], Jaroslaw Steciuk[b], Magdalena Zaborowska[b], Jakub M. Szurmak[b], Roman Dubianski[a],
6 Anna Maassen[b], Malgorzata Stachowiak[a], Bruno Huettel[c], Monika Ciesla[b], Klaudia Kogut[b], Anna
7 T. Rolicka[b,d], Saleh Alseekh[e,f], Ernest Bucior[b], Rainer Franzen[g], Anna Klepacz[b], Malgorzata A.
8 Domagalska[g], Samija Amar[g], Janusz A. Siedlecki[a], Alisdair R. Fernie[e,f], Seth J. Davis[g,h,i *^],
9 Tomasz J. Sarnowski[b*^]

10

11 [a] Maria Sklodowska- Curie National Research Institute of Oncology, Roentgena 5, Warsaw,
12 Poland
13 [b] Institute of Biochemistry and Biophysics Polish Academy of Sciences, Pawinskiego 5A
14 Warsaw, Poland
15 [c] Max Planck Genome Centre Cologne, D-50820 Cologne, Germany
16 [d] Faculty of Biology, University of Warsaw, Warsaw, Poland
17 [e] Max Planck Institute of Molecular Plant Physiology, 14476 Potsdam-Golm, Germany
18 [f] Center for Plant Systems Biology and Biotechnology, 4000 Plovdiv, Bulgaria
19 [g] Max-Planck Institute for Plant Breeding Research; D-50829 Cologne, Germany
20 [h] State Key Laboratory of Crop Stress Biology, School of Life Sciences, Henan University,
21 13 Kaifeng 475004, China
22 [i] Department of Biology, University of York, York YO10 5DD, UK

23

38   # shared first authorship

39   * senior authors

40   ^ address correspondence to:

41   **Tomasz J. Sarnowski** tsarn@ibb.waw.pl

42   **Seth J. Davis** seth.davis@york.ac.uk

43   **Corresponding authors:** Seth J. Davis and Tomasz J. Sarnowski

44   **Senior authors:** Seth J. Davis and Tomasz J. Sarnowski

45

Short title: The Role of ERECTA and SWI3B in GA Signaling

ONE SENTENCE SUMMARY: ERECTA leucine-rich receptor-like kinase and SWI3B subunit of SWI/SNF chromatin remodeling complex cooperate in direct transcriptional control of *GID1* genes in Arabidopsis.

Authors Contributions

TJS, ES, and SJD planned experiments and wrote the manuscript

SK and PC participated in the planning of some experiments

TJS, ES, SK, PC, SS, SA, BH, JAS, and ARF analyzed the data

ES, PC, SS, SK, PO, JS, MZ, JMS, RD, AM, MS, BH, MC, KN, ATR, EB, RF, AK, MAD, SA, and TJS performed experiments

All authors read, edited, and approved the final manuscript

Key Words: Arabidopsis, ERECTA, ERECTA-LIKE1, ERECTA-LIKE2, LRR-RLK, SWI/SNF, SWI3B, HER2, Chromatin

Abbreviations and Acronyms:

ERf, ERECTA family; ER, ERECTA; ERL1, ERECTA-LIKE 1; ERL2, ERECT-LIKE 2; LRR-RLKs, leucine-rich repeat receptor-like kinases; CRC, chromatin remodeling complex; SWI/SNF, Switch/Sucrose Nonfermenting; *GID1*, *GIBBERELLIN INSENSITIVE DWARF 1*; GA, gibberellin; PAC, Paclobutrazol; qRT-PCR, quantitative real-time PCR; BFA, Brefeldin A; NLS, nuclear localization signal; KDER, the kinase domain of ERECTA; TSS, transcription start site; EGFR, epidermal growth factor receptor.

Abstract

The Arabidopsis ERECTA family (ERf) of leucine-rich repeat receptor-like kinases (LRR-RLKs), comprising ERECTA (ER), ERECTA-LIKE 1 (ERL1) and ERECTA-LIKE 2 (ERL2), control epidermal patterning, inflorescence architecture, stomata development, and hormonal signaling. Here we show that the *er/erl1/erl2* triple mutant exhibits impaired gibberellin (GA) biosynthesis and perception alongside broad transcriptional changes. ERf proteins interact in the nucleus, *via* kinase domains, with the SWI3B subunit of the SWI/SNF chromatin remodeling complex (CRCs). The *er/erl1/erl2* triple mutant exhibits reduced SWI3B protein level and affected nucleosomal chromatin structure. The ER kinase phosphorylates SWI3B *in vitro*, and the inactivation of all ERf proteins leads to the decreased phosphorylation of SWI3B protein *in vivo*. Correlation between DELLA overaccumulation and SWI3B proteasomal degradation together with the physical interaction of SWI3B with DELLA proteins explain the lack of RGA accumulation in the GA- and SWI3B-deficient *erf* mutant plants. Co-localization of ER and SWI3B on *GID1* (*GIBBERELLIN INSENSITIVE DWARF 1*) DELLA target gene promoter regions and abolished SWI3B binding to *GID1* promoters in *er/erl1/erl2* plants supports the conclusion that ERf-SWI/SNF CRC interaction is important for transcriptional control of GA receptors. Thus, the involvement of ERf proteins in transcriptional control of gene expression, and observed similar features for human HER2 (Epidermal Growth Family Receptor-member), indicate an exciting target for further studies of evolutionarily conserved non-canonical functions of eukaryotic membrane receptors.

90 **Introduction**

91   The ERECTA family (ERf) of leucine-rich-repeat receptor-like kinases (LRR-RLKs)

92 consists of three members: ERECTA (ER), ERECTA-LIKE 1 (ERL1), and ERECTA-LIKE 2

93 (ERL2). ERf proteins carry extra-cellular leucine-rich repeats (LRRs), as well as transmembrane

94 and cytosolic kinase domains (Shpak et al., 2004; Torii et al., 1996, Kosentka et al., 2017).

95 Inactivation of *ERECTA* leads to inflorescence, pedicels, and siliques compaction, while the

96 individual loss of either *ERL1* or *ERL2* function has a limited effect on Arabidopsis development

97 (Shpak et al., 2004). ERf proteins are functionally redundant-their simultaneous inactivation

98 results in dramatic growth retardation, severe dwarfism, enlargement of the shoot apical meristem

99 (SAM), clustered stomata, and sterility. ERf regulates stem cell homeostasis *via* buffering

100 cytokinin responsiveness and auxin perception in SAM and modulating the balance between stem

101 cell proliferation and consumption (Shpak et al., 2004; Griffiths et al., 2006; Torii et al., 2007;

102 Chen et al., 2013; Shpak, 2013; Uchida et al., 2013; Zhang et al., 2021). ERECTA controls the

103 expression of genes associated with gibberellin (GA) metabolism (Uchida et al., 2012a)

104 restricting xylem expansion downstream of the GA pathway (Ragni et al., 2011). It additionally

105 regulates shade avoidance in a GA and auxin-dependent manner (Du et al., 2018) and

106 ethylene-induced hyponastic growth (Van Zanten et al., 2010).

107   Overexpression of ER variant lacking the C-terminal kinase domain (ERΔK) caused more

108 severe developmental defects than complete inactivation of *ERECTA,* suggesting an interaction

109 of the kinase domain with important regulatory partners (Shpak, 2003). ERECTA interacts with

110 ERL1 and ERL2 to form receptor complexes recognizing two endodermis-derived peptide

111 hormones (EPFL4 and EPFL6), regulating vascular differentiation and stem elongation. ERf

112 proteins additionally form complexes with the receptor-like protein TOO MANY MOUTHS

113 (TMM), which controls stomatal differentiation by recognition of the secretory peptides

114 EPIDERMAL PATTERNING FACTOR 1 (EPF1), EPF2, and stomagen (Lee et al., 2012;

115 Uchida et al., 2012a; Lee et al., 2015b).

116   ERL2 has been found to undergo endocytosis (Ho et al., 2016), suggesting that ERf

117 proteins may play, as yet uncharacterized, regulatory roles upon internalization, in addition to

118 their functions as ligand-binding membrane receptors. ERECTA signaling, in tandem with the

119 SWR1 chromatin remodeling complex (CRC), controls the expression of the *PACLOBUTRAZOL*

120 *RESISTANCE 1* (*PRE1*) family genes. This observation supports their role in the GA signaling

121   pathway, however, neither direct interaction between ERECTA and SWR1 nor the direct

122   influence of ERECTA signaling on chromatin structure or SWR1 activity has, as yet, been

123   demonstrated (Cai et al., 2017; Cai et al., 2021).

124   Here we show that the loss of all ERf proteins in the *er/erl1/erl2* triple mutant (*erf*) results

125   in broad transcriptomic changes affecting hormonal, developmental, and metabolic processes.

126   Inactivation of ERf proteins caused down-regulation of the GA receptor *GID1* (*GIBBERELLIN*

127   *INSENSITIVE DWARF 1*) genes expression and decreased bioactive GA levels. The ER protein

128   undergoes endocytosis and enters the nucleus. All three ERf proteins interact in the nucleus with

129   the SWI3B core subunit of the SWI/SNF CRCs. The kinase domain of the ER protein exhibits the

130   ability to phosphorylate SWI3B protein. The physical interaction of SWI3B with RGA and

131   RGL1, together with identified correlation between DELLA accumulation and SWI3B

132   proteasomal degradation, provide an explanation as to why GA-deficient *erf* mutant plants did

133   not overaccumulate RGA. These data collectively suggest cooperation of ERf-signaling with

134   SWI/SNF in the modulation of gene transcription. The ER and SWI3B also co-localized in the

135   promoter regions of *GID1* DELLA target genes. In the *erf* mutant, the binding of SWI3B to *GID1*

136   promoters was abolished. These results collectively suggest that ERf proteins directly control GA

137   receptor expression by restricting recruitment of the SWI/SNF CRCs to its target *loci*.

138

139 **Results**

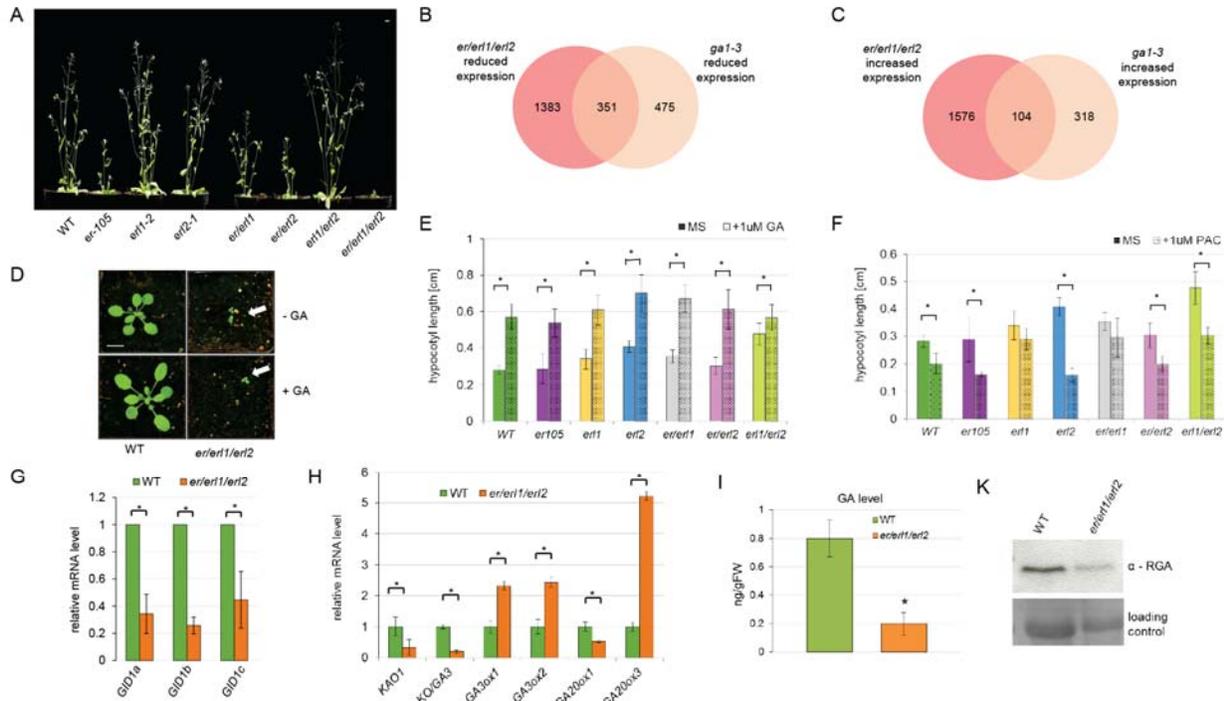140 **Inactivation of *Erf* Proteins Has a Broad Effect on the Arabidopsis Transcriptome**

141 **including GA Signaling.**

142   The Arabidopsis *er/erl1/erl2* plants exhibit severe dwarfism, dark green color, defects in

143 vascular development, stem elongation, and stomatal differentiation, as well as complete sterility

144 (Figure 1 A, Supplemental Figure 1A, (Shpak et al., 2004)).

145

Figure 1. *ERf* inactivation affects Arabidopsis development, causes transcriptomic changes overlapping with the effect of *ga1-3* mutation and impairs GA biosynthesis and signaling (See also Figures S1, S2 and S3). A, Phenotypic changes conferred by combinations of *erf* mutations. Scale bar= 1 cm. B, Overlapping down-regulated genes in *er/erl1/erl2* and *ga1-3* plants. C, Overlapping up-regulated genes in *er/erl1/erl2* and *ga1-3* plants. D, The *er/erl1/erl2* plants exhibit impaired GA response. 14-days old LD (12h day/12 night) grown WT and *er/erl1/erl2*, sprayed twice a week with water (upper row) or 100µM GA$_{4+7}$ (lower row). Arrows-*er/erl1/erl2* plants. Scale bar= 1cm. E, The GA response is retained to various levels in combinations of *erf* mutants. Error bars-SD,* = P < 0.05, Student's *t*-test, *n*= 30 plants. F, The response of various *erf* mutants to 1µM Paclobutrazol treatment. Error bars-SD,* = P < 0.05, Student's t test, n= 30 plants. G, The *er/erl1/erl2* mutant exhibits altered transcription of *GID1* GA receptor genes (error bars-SD, P < 0.05, Student's *t*-test, three biological and technical replicates were assayed). H, The *er/erl1/erl2* mutant displays altered GA biosynthesis and metabolism-related genes expression (error bars-SD, P < 0.05, Student's *t*-test, three biological and technical replicates were assayed). I, The *er/erl1/erl2* mutant exhibits dramatically reduced level of bioactive GA$_{4+7}$ gibberellin (error bars-SD, P < 0.05, Student's *t*-test, three biological and technical replicates were assayed). J, The *er/erl1/erl2* mutant shows decreased level of the DELLA protein RGA.

165   Given the severe phenotypic alterations of the *er/erl1/erl2* plants, we performed transcript

166   profiling with Affymetrix ATH1 microarrays on RNA samples from aerial parts of the

167   *er/erl1/erl2* mutant and WT (wild type) adult plants (representing the most comparable stage of

168   the development) grown for 5 weeks under long-day conditions (16h day/8h night). Data analysis

169   identified 1734 versus 1680 genes showing >1.50-fold decrease and increase, respectively, of

170   transcript levels in *er/erl1/erl2* comparing to WT (Supplemental Figure 1B, Supplemental

171   Dataset 1 Sub-tables 1, 2). Gene Ontology (GO) terms of primary metabolism, developmental

172   processes, and response to hormones were enriched among the *er/erl1/erl2* down-regulated genes

173   (Supplemental Dataset 1 Sub-table 3). Among these, 27 genes were classified to GA-response

174   (Supplemental Table 1, Supplemental Dataset 1 Sub-tables 1, 3). The up-regulated genes were

175   classified into GO-terms of chloroplast-related metabolic and light-regulated transcription

176   processes, responses to cytokinin, and auxin degradation (Supplemental Dataset 1 Sub-Tables

177   2,4). Several genes acting in leaf epidermal and stomatal cell differentiation showed enhanced

178   transcription in the *er/erl1/erl2* mutant (Supplemental Table 2). In conclusion, the inactivation of

179   ERf altered transcriptional regulation of hundreds of targets, including a set of GA-regulated

180   genes.

181   Phenotypic traits exhibited by double and triple *erf* mutants resemble those of double and

182   triple *gid1abc* (*gibberellin insensitive dwarf 1a, b* and *c*) plants (Figure 1A; (Griffiths et al.,

183   2006)). Inactivation of *GID1abc* genes has a nearly identical effect on the Arabidopsis

184   transcriptome as the severe GA-deficient mutant *ga1-3* (Willige et al., 2007), thus we compared

185   the transcriptomic data available for the *ga1-3* mutant with those caused by inactivation of all *ERf*

186   genes.

187   We identified a large overlap of differentially expressed genes (DEG) in the *er/erl1/erl2*

188   and *ga1-3* lines. Among 826 genes down-regulated in the *ga1-3* line, 351 (about 42.5%) also

189   exhibited decreased expression in the *er/erl1/erl2* plants (Figure 1B), while 104 genes (about

190   24.6% of *ga1-3* up-regulated genes) were up-regulated in both lines (Figure 1C). Only 33 genes

191   were up-regulated in *ga1-3* but down-regulated in *er/erl1/erl2* (Supplemental Figure 1C), and

192   only 64 genes down-regulated in *ga1-3* but up-regulated in *er/erl1/erl2* (Supplemental Figure

193   1D). DEG common to *ga1-3* and *er/erl1/erl2* lines belonged to both DELLA (repressors of GA

194   pathway) -dependent and DELLA-independent classes (Cao et al., 2006), regardless of whether

195   they display co-regulation or contrasting regulation in these lines (Supplemental Figure 1E and

196   F). This suggests the involvement of Arabidopsis ERf proteins in the control of GA-related

197   processes. Therefore, we next tested the response of *er/erl1/erl2* plants to exogenously supplied

198   bioactive 100 µM GA$_{4+7}$ and found that spraying of the *er/erl1/erl2* mutant grown under LD

199   condition (12h day/12h night) did not lead to increased leaf size by day 14 compared to the

200   remarkable expansion of control WT rosette leaves (Figure 1D, Supplemental Figure 2A). Thus

201   *er/erl1/erl2* displayed GA insensitivity. Nonetheless, the GA-treatment resulted in bolting of

202   *er/erl1/erl2* plants, only after over two months (Supplemental Figure 2B and C), indicating their

203   residual response to GA.

204   Although we showed that ERf proteins are involved in the GA response, it remained

205   unclear whether proper GA perception requires all ERf proteins. Thus, we tested the hypocotyl

206   response of single and double *erf* mutants in various combinations to the treatment with 1 µM

207   GA$_{4+7}$ or 1 µM Paclobutrazol (PAC), an inhibitor of GA biosynthesis. The GA response was

208   retained to various levels in all tested mutants (Figure 1E) while the *erl1* and *er/erl1* plants had an

209   impaired response to PAC and *erl1/erl2* displayed a significant reduction of hypocotyl length

210   (Figure 1F).

211   Upon crossing *er*, *er/erl1*, and *er/erl2* lines with the *ga1-3* mutant, we observed only a

212   discrete enhancement of the *ga1-3* phenotype. However most of the phenotypic changes

213   characteristic for *ga1-3* mutation were retained, indicating that many of the *er, erl1,* or *erl2* single

214   or double mutant phenotypes are likely not exclusively a result of GA deficiency (Supplemental

215   Figure 2D and E).

216   We have proven that only parallel inactivation of all ERf proteins causes severe

217   impairment of the GA response. Quantitative real-time PCR (qRT-PCR) measurements of GA

218   response and biosynthesis genes expression revealed a parallel 2.5 to 3-fold reduction in the

219   transcript levels of all three *GID1* GA-receptors in the *er/erl1/erl2* mutant compared to WT

220   (Figure 1G). The GA-receptor genes *GID1A/B* have been reported to be direct ChIP targets of

221   RGA, a major DELLA repressor of GA-signaling, which stimulates *GID1* transcription (Zentella

222   et al., 2007). The *er/erl1/erl2* triple mutant also displayed altered expression of GA biosynthesis

223   genes compared to the WT: a 4-fold reduction of mRNA levels of *KAO1* (*ent*-kaurenoic acid

224   oxidase) and *KO* (*ent*-kaurene oxidase), a 2.5-fold increase of mRNA levels of GA-repressed

225   *GA3ox1* and *GA3ox2* (GIBBERELLIN 3 BETA-HYDROXYLASE 1 and 2), a 2-fold inhibition

226   and 5-fold up-regulation, respectively, of mRNA levels corresponding to the *GA20ox1* and
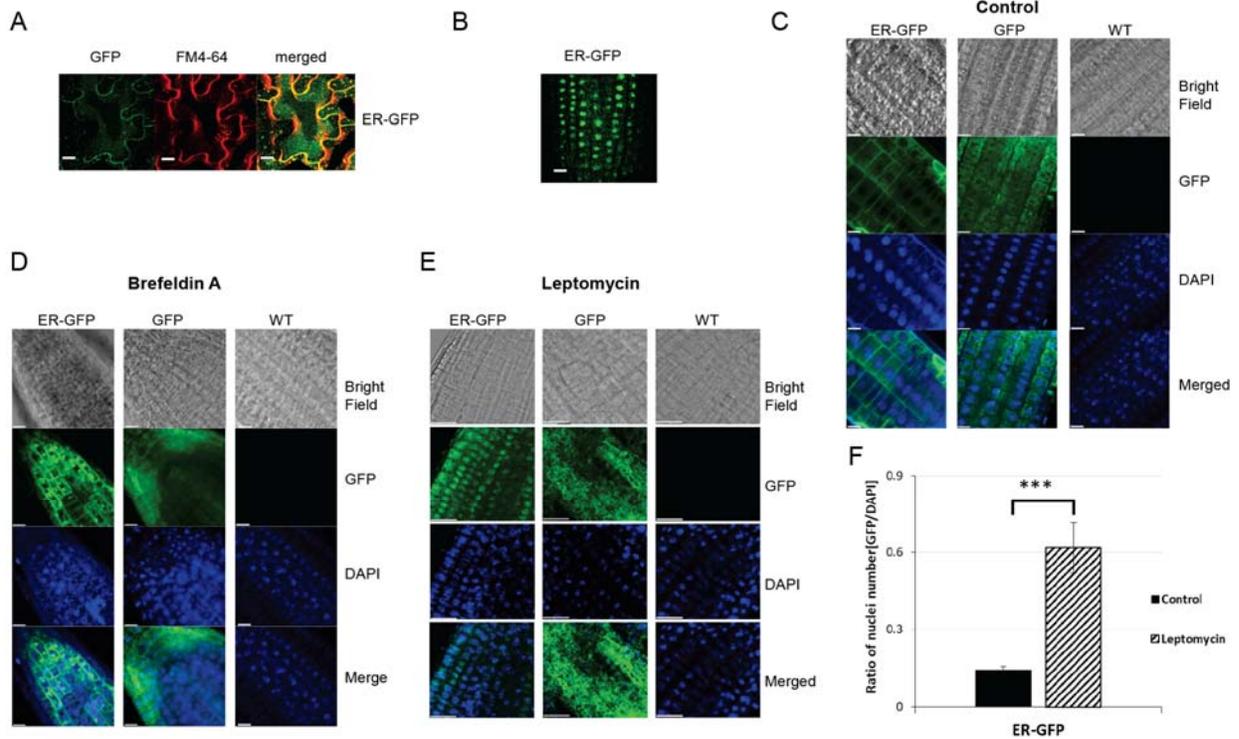
227   *GA20ox3* genes (Figure 1H). This indicated that the ERf proteins not only influence the

228   expression of GA receptors, but also genes associated with GA biosynthesis. We subsequently

229   found a substantial decrease of bioactive GA_4 as well as GA_{12}, and GA_{24} intermediates in

230   *er/erl1/erl2* mutant (Figure 1I, Supplementary Figure 3). Counterintuitively, the Western blotting

231   using a specific antibody (Willige et al., 2007) detected reduced levels of RGA in the *er/erl1/erl2*

232   mutant plants (Figure 1J). Our results indicate that the parallel inactivation of all ERf proteins

233   results in co-ordinate deregulation of GA biosynthesis and response pathways in Arabidopsis.

234

235   **ERECTA (ER) Protein Undergoes Endocytosis and Migrates to the Nucleus.**

236   In analogy to some human membrane receptors internalizing to endosomes and migrating

237   to the nucleus (*i.e.,* Giri et al., 2005), the ERL2 member of the ERf undergoes endocytosis (Ho et

238   al., 2016). We next examined, in detail, the cellular localization of ER by creating C-terminal

239   GFP fusions with ER (Figure 2A) after verifying genetic complementation of the *er-105* mutation

240   by a 35S::ER-GFP construct (Supplemental Figure 4).

241

Figure 2. Subcellular localization of ERECTA protein (See also Figures S4 and S5). A, ERECTA is localized in plasma-membrane and endosomes in epidermal cells of 7-days old seedlings. ER-GFP, or free GFP visualized using GFP channel. FM4-64 specifically stains plasma-membranes. Scale bar=10µm. B, Root-tip images of approximately two-week-old (14-17 days) ER-GFP seedlings showing nuclear localization of ERECTA protein at considerable frequency. C, Root-tip images of 12-day-old ER-GFP seedlings serving as the control for D and E. D, Brefeldin A treatment enhanced the localization of ERECTA protein in Brefeldin A (BFA) bodies. Roots of 12-day-old Arabidopsis seedlings. E, Leptomycin B treatment enhanced the nuclear localization of ERECTA Free GFP was used as a control in C, D, and E, cell nuclei were stained with DAPI, scale bar= 50µm. F, Letomycin B enhances nuclear presence of ER protein. The GFP/DAPI ratio calculated per area for roots of plants expressing ER-GFP protein.

255   As observed earlier (Shpak et al., 2005; Uchida et al., 2012a), a pool of the ER-GFP
256   protein was detected in association with plasma-membranes of the leaf epidermis. In addition, a
257   weak localization signal was detected in internal structures, which could represent endosomes
258   (Figure 2A). In guard cell pairs, ER-GFP protein was also detected in circles around the positions
259   of nuclei, which were visualized by propidium iodide staining (Supplemental Figure 5A and
260   Supplemental Movie 1). We also observed with considerable frequency ER protein in the nuclei
261   of roots of 14- to 17-day-old Arabidopsis plants (Figure 2B), however ER was mainly located in
262   the plasma membrane and endosome-like structures (Figure 2C).

263   To verify that the ER-GFP protein indeed undergoes endocytosis, we examined its
264   localization in Arabidopsis seedlings treated with 25μM Brefeldin A (BFA), a compound
265   preventing Golgi-mediated vesicular transport of membrane proteins to the plasma membrane
266   (Miller et al., 1992). We observed accumulation of the ER-GFP protein in BFA bodies within 30-
267   40 min after BFA treatment leading to its accumulation at the nuclei periphery 120 min after
268   BFA application (Figure 2D, Supplemental Figure 5B). The 4h long 200 nM leptomycin B
269   treatment (a compound blocking nuclear export by EXPORTINS (Haasen et al., 2002)) resulted
270   in the ER accumulation in the cell nuclei (Figure 2E, F). ER thus appeared to behave similarly to
271   certain human plasma-membrane receptors in migrating into the nucleus (Hung et al., 2008; Chen
272   and Hung, 2015).

273   We noted that ERL1 and ERL2 proteins carry a monopartite nuclear localization signal
274   (NLS) sequence in their kinase domains, while the ERL1 kinase domain carries an additional
275   bipartite NLS identified using cNLS Mapper (Kosugi et al., 2009b). The NLS signal in the ER
276   protein was not recognized, however, all ERf proteins show evolutionarily conserved amino acid
277   sequences in this region (Supplemental Figure 6A). Using the NetNES1.1 (la Cour et al., 2004)
278   server, we predicted the existence of specific for AtXPO1/AtCRM1 exportin (Haasen et al.,
279   2002) leucine-rich nuclear export signals (NES) in all ERf proteins (Supplemental Figure 6A).
280   The subsequent Western-blotting analysis of nuclear extracts (Supplemental Figure 6B)
281   confirmed the nuclear presence of ER. In addition to the expected full-length forms (140 kDa),
282   we also detected shorter (~75 kDa) versions of the ERECTA protein with the C-terminal GFP tag
283   and smaller products of degradation, including free GFP, suggesting an analogy to the human
284   Epidermal Growth Factor Receptor (EGFR), (Chen and Hung, 2015). The detection of N-
285   terminally truncated forms of the ERECTA protein carrying a kinase domain resembled the

286   recently reported fate of the XA21 LRR-RLK immune receptor in rice (Park and Ronald, 2012),

287   where its C-terminal kinase domain enters the nucleus to interact with the OsWRKY62

288   transcriptional regulator.

289   To assess whether the ERECTA kinase domain (KDER) is imported into the nucleus, we

290   fused the C-terminal part of ERECTA, harboring the KDER, to a YFP-HA tag (Supplemental

291   Figure 6C) and expressed this construct in the *er-105* mutant. The presence of KDER-YFPHA

292   was detected exclusively in cell nuclei (Figure 3A). Furthermore, KDER-YFPHA expression

293   partially restored the *er-105* rosette and cauline leaf phenotype to WT values (Supplemental

294   Figure 7A, B). Still, it failed to genetically complement the defect of stem elongation

295   (Supplemental Figure 7C). Partial genetic complementation of the *er-105* mutation and nuclear

296   localization of KDER prove that the KDER has a receptor-domain independent signaling

297   function. Interestingly, by contrast to the full length and kinase domain of ERECTA protein

298   (Figure 3A), truncated ERΔkinase form of ERECTA protein fused to YFP-HA (ΔKDER-YFP-

299   HA) did not enter into the nucleus proving the presence of functional NES and NLS sequences in

300   the C-terminal part of ERECTA protein.

301

302
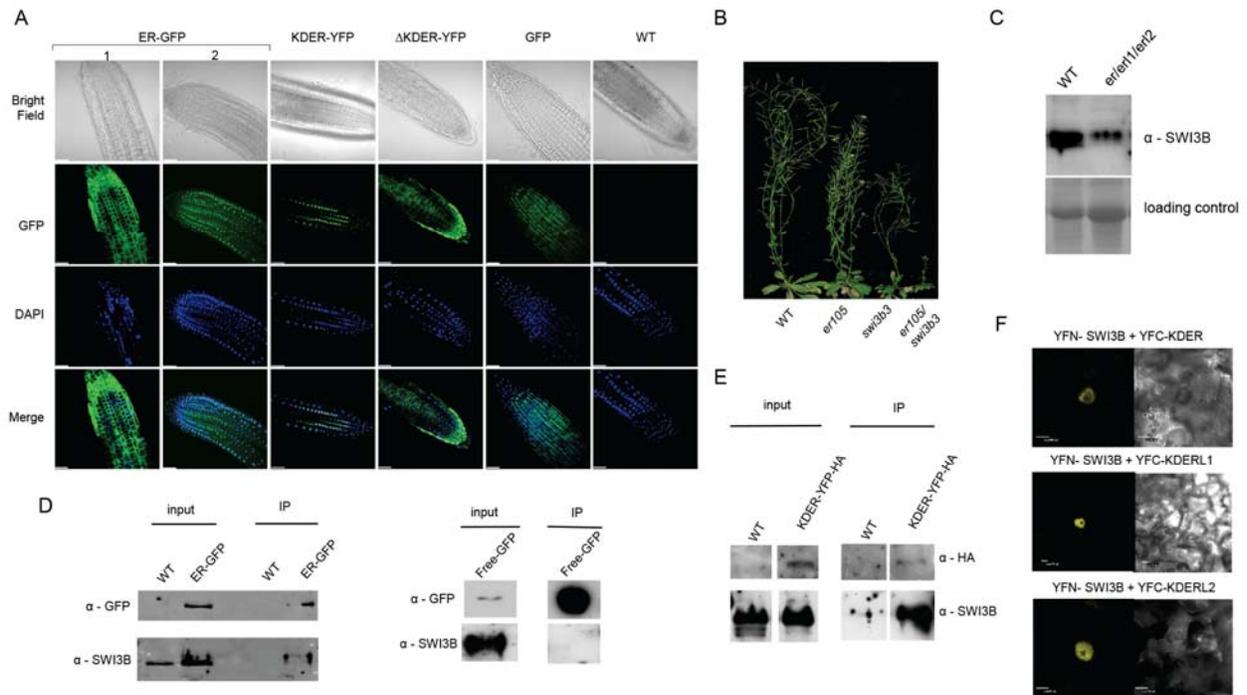
303

304 **Figure 3.** Nuclear function of ERf proteins (See also Figures S6, S7, S8, S9, and S10). A, Root-
305 tip images of approximately two-week-old (14-17 days) plants expressing ER-GFP, KDER-YFP-
306 HA (the kinase domain of the ER protein), ERΔK-YFPHA (truncated ER protein lacking the
307 kinase domain) proteins indicating that the kinase domain is necessary for the nuclear localization
308 of ER protein. WT and GFP expressing plants-negative controls. Panel 2 in the ER-GFP indicates
309 nuclear localization of ER protein appearing at considerable frequency. Cell nuclei were stained
310 with DAPI. Scale bar=25 μm. B, The *er-105/swi3b3* double mutant shows more retarded growth
311 than either *er-105* or *swi3b3* plants. Scale bar= 1cm. C, The *er/erl1/erl2* triple mutant exhibits
312 reduced SWI3B protein level. D, ER-GFP or free GFP (negative control) pull-down from the
313 nucleus and anti-SWI3B western blotting indicate a specific ER-SWI3B interaction. E,
314 Immunoprecipitation of KDER-YFP-HA from the nucleus indicated that the kinase domain of
315 ER interacts with SWI3B. F, ER, ERL1, and ERL2 kinase domains interact with SWI3B in the
316 nucleus. Bimolecular Fluorescence Complementation assay (BiFC) in epidermis of tobacco
317 leaves. Scale bar = 10μm.

318

319   Upon nuclei fractionation (Sarnowski et al., 2002), the ERECTA protein was detected in
320   the nuclear membrane, soluble nuclear-protein fraction, and chromatin, with its major presence
321   within the nuclear matrix. The nuclear fractions contained both full-length and N-terminally
322   truncated ER forms (Supplemental Figure 8) suggest that ER could be involved in either
323   transcriptional regulation or other nuclear functions.

324

325   **ERf Proteins Physically Interact with the SWI3B Core Subunit of SWI/SNF CRC**

326   The weak *swi3b-3* allele (Sáez et al., 2008) carrying, in the *er-105* background, a point
327   mutation in the *SWI3B* gene encoding a core subunit of the SWI/SNF chromatin remodeling
328   complex (CRC) exhibit severe dwarfism, altered leaf shape, delayed flowering and reduced
329   fertility (Figure 3B). We, therefore, introgressed the *swi3b-3* mutation into WT and found that the
330   phenotypic alterations related to *swi3b-3* were much weaker (slight reduction of growth rate,
331   leading to decreased plant height, Figure 3B) than the phenotypic traits exhibited by the *er-
332   105*/*swi3b-3* as well as single *er-105* mutation. The severe phenotypic alterations exhibited by the
333   *er-105*/*swi3b-3* plants indicated the likely existence of a strong genetic interaction between the
334   ERECTA signaling pathway and SWI3B-containing SWI/SNF CRCs. This observation is in line
335   with *i)* the direct binding of 15 out of 27 potential ERf target genes related to the GA signaling
336   pathway (Supplemental Table 1) by SWI/SNF CRCs (Sacharowski et al., 2015; Archacki et al.,
337   2016; Li et al., 2016); *ii)* the unexpected broad transcriptional changes and severe effects on
338   Arabidopsis development and hormonal signaling pathways observed in the *er/erl1/erl2* mutant,
339   and *iii)* the well-recognized function of SWI/SNF CRC in hormonal crosstalk including GA
340   signaling (Sarnowska et al., 2013; Sarnowska et al., 2016).

341   We next assessed the level of the SWI3B protein in *er/erl1/erl2* plants. We found a
342   significant decrease in the SWI3B protein abundance (Figure 3C), further suggesting that the ERf
343   signaling pathway may influence the proper function of SWI3B-containing SWI/SNF CRCs.
344   Additionally, the SWI3B was found to bind ER-GFP but not free GFP (Figure 3D). Similarly, co-
345   immunoprecipitation indicated that SWI3B interacts with the kinase domain of ER (Figure 3E).

346   Next, we performed BiFC assays (Hu et al., 2002) in epidermal cells of *Nicotiana
347   benthamiana* and confirmed the SWI3B and ER kinase domain interaction. The YFC-RFP served
348   as a control unrelated protein with broad intracellular localization (Figure 3F, Supplemental
349   Figure 9). We also detected the interaction of SWI3B with the kinase domain of the ERL1 or
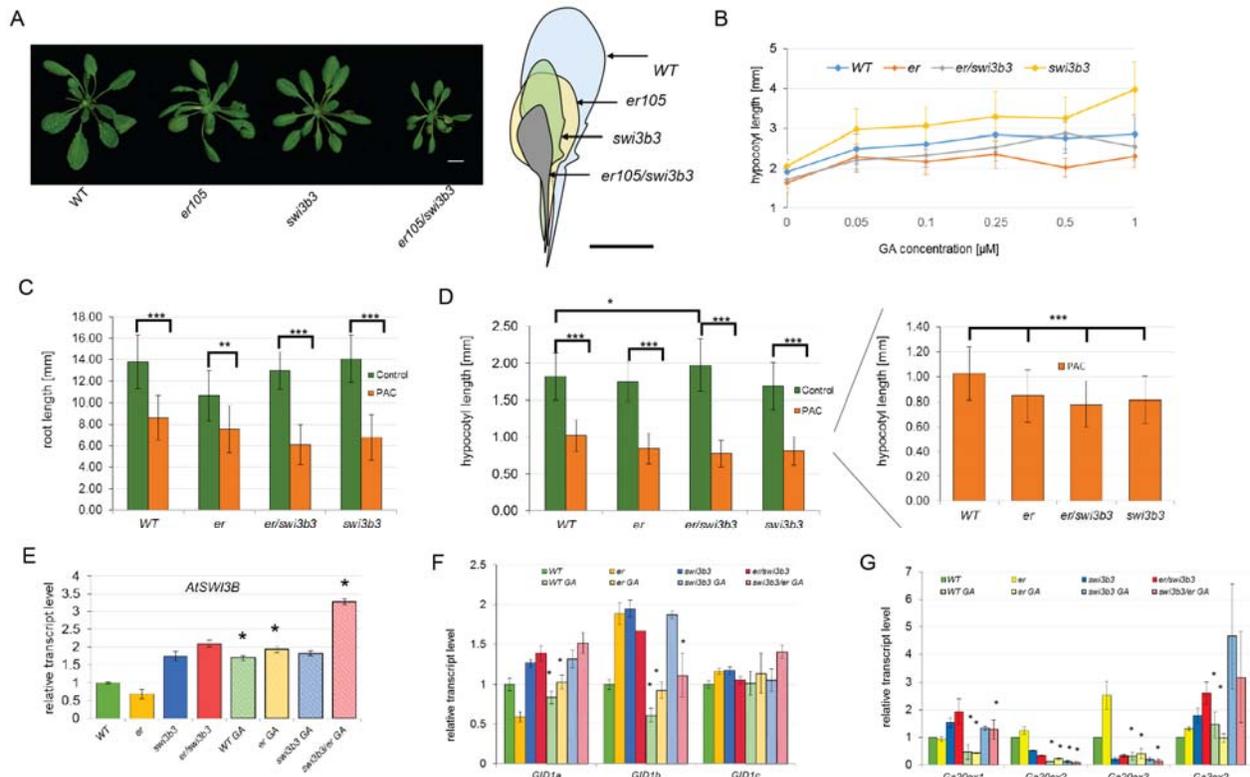
350   ERL2 (Figure 3F, Supplemental Figure 9), indicating the existence of direct interdependences

351   between the ERf signaling pathway and SWI/SNF–dependent chromatin remodeling.

352   Moreover, we found similar interactions in the nuclei of human cells for HER2

353   (Epidermal Growth Factor Receptor- family member), a membrane receptor acting in a non-

354   canonical signaling mode including translocation to the nucleus (Lee et al., 2015a), and BAF155

355   a SWI3-type subunit of human SWI/SNF CRCs (Supplemental Figure 10). Thus, our data

356   indicate that the phenomenon observed for ERf and SWI3B is not limited to Arabidopsis but

357   rather may be a general feature of SWI/SNF CRCs and membrane receptors.

358

359   ***ERECTA* and *SWI3B* Interact Genetically and *er/elr1/erl2* Plants Exhibit Alteration in**

360   **Chromatin Status.**

361   The *er-105/swi3b-3* double mutant exhibited more severe phenotypic traits than both single *er-*

362   *105* and *swi3b-3* mutant lines (Figure 4A), supporting the observed physical interdependences

363   between ER and SWI3B.

364

Figure 4. ER and *SWI3B* interact genetically and affect both GA biosynthesis and response pathways (See also Figures S11 and S12). A, The *er-105/swi3b-3* double mutant exhibits more retarded growth than the *er-105* and *swi3b-3* (three-weeks old plants). Graphical alignment of corresponding leaves. Scale bar= 1 cm. B, The hypersensitivity of 1-week-old *swi3b-3* hypocotyl to GA treatment is abolished by introducing *er-105*. C, Roots of all tested 1-week-old genotypes similarly respond to PAC treatment (error bars-SD, *P < 0.01,** P < 0.001, ***P<0.0001, Student's *t*-test). D, Hypocotyls of all tested 1-week-old genotypes similarly respond to PAC treatment, right panel- hypocotyl length comparison for PAC treated plants only (error bars-SD, *P < 0.01,** P < 0.001, ***P<0.0001 Student's *t*-test). E, *swi3b-3* weak, point mutant line and *er-105/swi3b-3* exhibit elevated *SWI3B* transcript level, the *SWI3B* expression is elevated after supplementation with bioactive GA$_{4+7}$ in all genotypes except *swi3b-3* (error bars-SD, P < 0.05, Student's *t*-test). F, The examination of *GID1* genes indicated that almost all examined lines responded to GA treatment, but the *swi3b-3* line was insensitive for GA-induced transcriptional changes (error bars-SD, P < 0.05, Student's *t*-test). G, The examination of GA biosynthesis genes indicated that almost all examined lines responded to GA treatment, but the *swi3b-3* line was insensitive for GA-induced transcriptional changes except *GA20ox2* expression (error bars-SD, P < 0.05, Student's *t*-test).

383

384 The treatment with bioactive GA_{4+7} gibberellins indicated hypersensitivity of *swi3b-3* to GA

385 demonstrated by hypocotyl length, while the response of *er-105* was reduced. By contrast, the

386 GA hypersensitivity of *swi3b-3* was abolished by introduced *er-105* mutation (Figure 4B). All

387 tested genotypes were responding to PAC treatment in a similar way (Figure 4C, D). The higher

388 expression of *SWI3B* was visible in the case of the *swi3b-3* mutant, which was even more

389 pronounced in *er-105/swi3b-3*. The expression of *SWI3B* was elevated after supplementation with

390 bioactive GA_{4+7} in all genotypes, except for the *swi3b-3* line (Figure 4E). The examination of

391 *GID1* and GA biosynthesis genes indicated that almost all examined lines responded to GA

392 treatment while the *swi3b-3* line was insensitive for induced by GA transcriptional changes

393 except for *GA20ox2* expression (Figure 4F, G). Collectively, our results further indicate that both

394 ERf signaling and SWI3B-containing CRCs play together an important role in the fine-tuning of

395 GA signaling in Arabidopsis.

396 To verify the biological effect of observed interactions between ERf signaling and SWI3B-

397 SWI/SNF, we analyzed the chromatin status, nuclei shape and chromocenters number in the

398 *er/erl1/erl2* mutant plants. We found that *er/erl1/erl2* plants exhibit increased chromocenter

399 number and altered spindle-like nuclei shape (Supplemental Figure 11A, B). We furthermore

400 screened the effect of inactivation of ERfs on genome-wide nucleosome positioning in chromatin

401 using *micrococcal nuclease* protection assays followed by deep sequencing (MNase-seq) and

402 confirmatory MNase-qPCR in WT and *er/erl1/erl2* plants.

403 We found that inactivation of ERf proteins has a broad influence on the global

404 nucleosomal chromatin structure in Arabidopsis- *erf* exhibited 41519 nucleosome occupancy

405 changes, 13924 "fuzziness" changes and 4055 nucleosome position changes (Supplemental

406 Figure 12A) and alterations in the presumable regulatory regions upstream of the transcription

407 start site (TSSs) (Supplemental Figure 12B, Supplemental Dataset 1, Sub-Table 9-14).

408 Among genes with down-regulated expression and altered nucleosome positioning in the

409 *er/erl1/erl2* mutant were 14 GA-related genes (*ATBETAFRUCT4, XERICO, PRE1, MYBR1,*

410 *MYB24, MIF1, HAI2, ZPF6, GA20ox1, CGA1, XTH24, GID1b, RGL1,* and *GIS3*) Interestingly,

411 seven of them (*ATBETAFRUCT4, PRE1, MYBR1, MIF1, XTH24, GID1b,* and *RGL1*) were

412 already observed to be directly targeted by the BRM ATPase of the SWI/SNF CRC (Archacki et
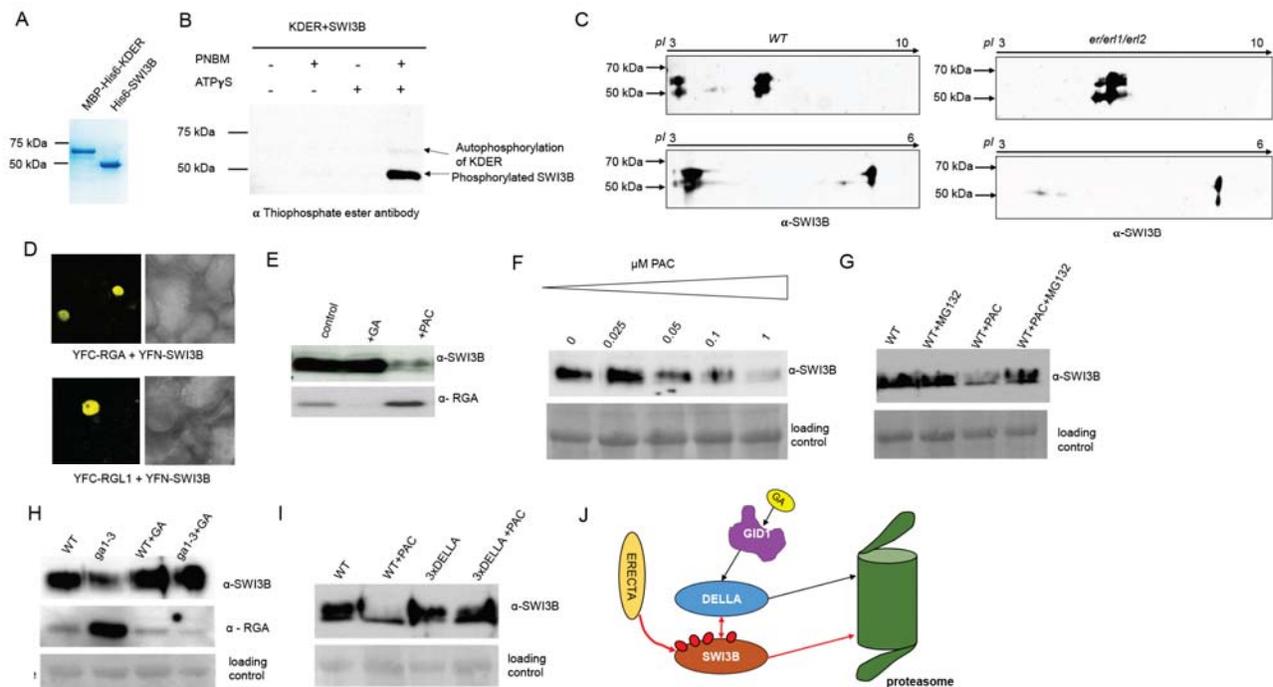
413 al., 2016; Li et al., 2016).

414   An Integrated Gene Browser (IGB) view of *PRE1, GID1a,b* promoter regions indicated

415   (Supplemental Figure 12D) various nucleosome alterations on promoter regions of these genes in

416   the *er/erl/erl2* mutant pointing out impaired chromatin remodeling in the absence of functional

417   ERf proteins. The selected changes were confirmed by MNase-qPCR (Supplemental Figure 12E).

418

419   **The Inactivation of ERf proteins Affects SWI3B Protein Phosphorylation**

420   We tested the ability of KDER to phosphorylate SWI3B protein. We overexpressed,

421   purified, and subsequently used MBP-His6-KDER and His6-SWI3B (Figure 5A, Supplemental

422   Figure 13A) for non-radioactive *in vitro* kinase assay. The existence of a strong band

423   corresponding to phosphorylated SWI3B protein and a weaker band of autophosphorylated

424   KDER was indicated (Figure 5B, Supplemental Figure 13B, C). The confirmatory mass-

425   spectrometry analysis resulted in the identification of the active phosphorylation sites at KDER

426   and in the SWI3B protein (Supplemental Figure 13D, E). Interestingly three of four KDER-

427   dependent phosphorylation sites were located in SWI3B in SWIRM and SANT domains

428   (Supplemental Figure 13E, F), providing a valuable hint that the ERf family proteins may be

429   responsible for the SWI3B phosphorylation.

430

Figure 5. ERf proteins are responsible for the phosphorylation of SWI3B protein, while DELLA proteins control SWI3B protein abundance (See also Figures S13, S14, and S15). A, Coomassie staining of MBP-His6-KDER and His6-SWI3B proteins purified from bacteria. B, Western blot with anti-Thiophosphate ester antibody (ab92570; Abcam) showing *in vitro* SWI3B phosphorylation by KDER. C, 2D Western blot assay with anti SWI3B antibody indicating *in vivo* phosphorylation alteration of SWI3B protein in *er/erl1/erl2* mutant. D, SWI3B and RGA and RGL1 proteins in the nuclei of living cells. Bimolecular Fluorescence Complementation assay (BiFC) in epidermis of tobacco leaves. Scale bar = 10µm. E, The amounts of SWI3B and RGA proteins in plants are oppositely regulated by PAC treatment. F, The disappearance of SWI3B protein is PAC-dose dependent. G, The PAC-dependent degradation of SWI3B is abolished by the MG132 treatment, a known proteasome inhibitor. H, The *ga1-3* mutant constitutively accumulating DELLA proteins exhibits the decreased level of SWI3B, which is restored to WT levels upon GA treatment. I, The triple DELLA mutant exhibits a WT-like level of SWI3B protein, and the PAC treatment does not influence SWI3B level in this background. J, Schematic model highlighting ERf and DELLA impact on the SWI3B protein.

448   To verify this possibility the *in vivo* phosphorylation analysis using 2D-IEF-PAGE

449   combined with the Western blot was performed. The alteration in the SWI3B proteins isoelectric

450   point (*pI*) in *er/erl1/erl2* mutant was observed. The bands corresponding to phosphorylated

451   SWI3B form were nearly absent in *er/erl1/erl2* plants, indicating a severe defect in SWI3B

452   phosphorylation (Figure 5C). This data strongly supports the regulatory function of the ERf

453   proteins on the SWI3B subunit of SWI/SNF CRC.

454

455   **Accumulation of DELLA Proteins Correlates with Increased Proteasomal Degradation of**

456   **SWI3B**

457   Our previous study demonstrated that SWI3C, a partner of SWI3B, physically interacts

458   with DELLA proteins (Sarnowska et al., 2013). We also found that the Arabidopsis lines with

459   impaired SWI/SNF CRCs- *brm* and *swi3c* exhibit decreased level of bioactive GA_4 gibberellins

460   level (Sarnowska et al., 2013; Archacki et al., 2013), but they do not accumulate RGA DELLA

461   protein similarly as in case of *er/erl1/erl2* plants (Supplemental Figure 14 and Figure 1J). To

462   address this unusual phenomenon, we used a BiFC assay to analyze the interaction between

463   DELLA and SWI3B. The interaction between either RGA or RGL1 protein and SWI3B was

464   found (Figure 5D, Supplemental Figure 15). No YFP signal was detected in control cells.

465   To understand the functional consequences of the detected interactions between SWI3B

466   and DELLA proteins, we analyzed the amounts of SWI3B and RGA proteins in GA or PAC-

467   treated plants (Figure 5E). Surprisingly, we observed the PAC-dose-dependent disappearance of

468   SWI3B protein (Figure 5F). To check if the degradation of SWI3B under these conditions

469   depended on the proteasome, we tested the effect of MG-132 on the SWI3B level. MG-132

470   treatment caused increasing SWI3B abundance in PAC treated plants (Figure 5G), suggesting

471   that the degradation of SWI3B observed in parallel to accumulation of DELLAs occurs *via* the

472   proteasome. We also observed increased degradation of SWI3B in the *ga1-3* mutant in which

473   DELLA proteins are constitutively accumulated (Figure 5H), but we did not observe enhanced

474   SWI3B degradation in PAC-treated 3xDELLA (Archacki et al., 2013) collectively suggesting

475   that binding of SWI3B by DELLA proteins may be a primary cause of its proteasomal

476   degradation (Figure 5I, J). Thus, the accumulation of DELLA proteins should lead to the same

477   consequences as the elimination of SWI3B protein or SWI3B-containing SWI/SNF CRCs. This

478   conclusion is strongly supported by the lack of RGA protein accumulation in GA deficient *brm*

479   and *swi3c* lines with inactivated other subunits of SWI/SNF CRC (Archacki et al., 2013;

480   Sarnowska et al., 2013). Therefore, it could be indeed expected that GA and SWI3B-deficient

481   *er/erl1/erl2* mutant will also not accumulate RGA protein because, in the case of SWI/SNF CRC

482   impairment, the DELLA accumulation seems to be irrelevant. Collectively, our results provide

483   new insight into the functioning of the ERECTA family proteins and DELLA proteins and their

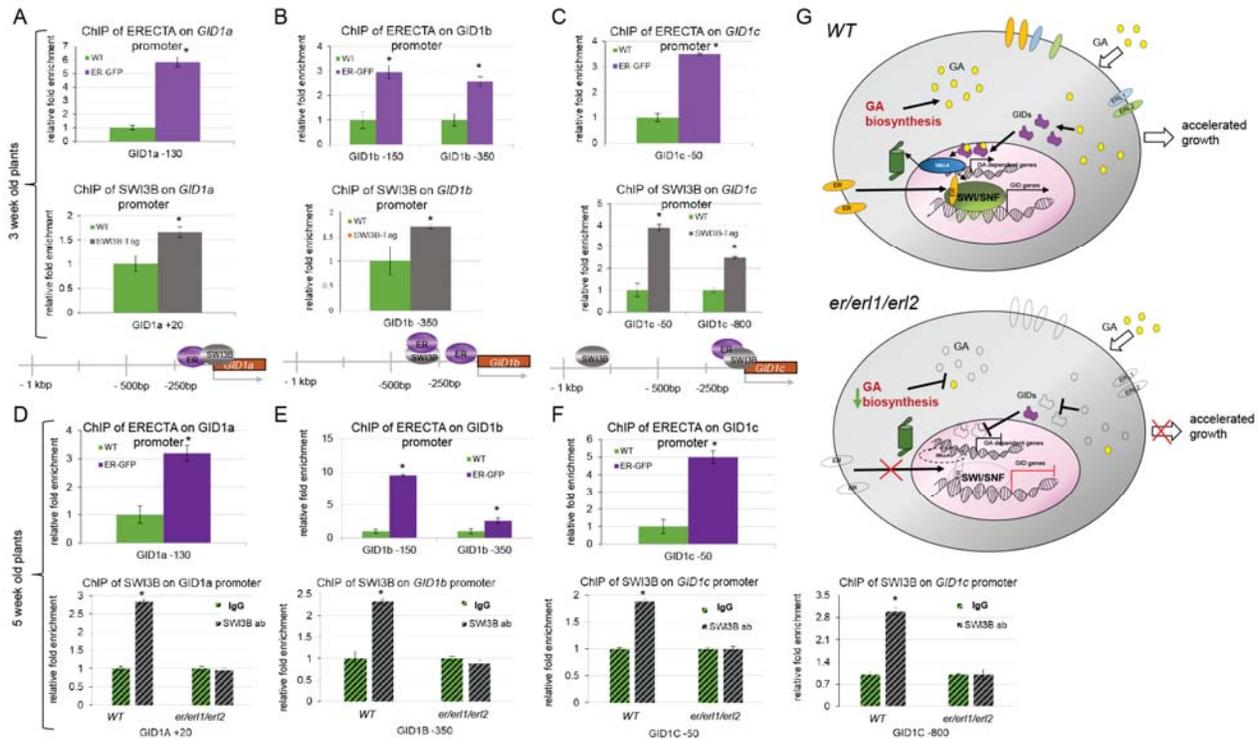484   mutual impact on the SWI3B-containing SWI/SNF CRCs.

485

486   **Binding of ERECTA and SWI3B to Promoter Regions of the *GID1* Genes**

487   The *er/erl1/erl2* mutant displays an impaired response to exogenous GA treatment and a

488   consistently decreased expression of all three *GID1* genes. ERf proteins interact with the SWI3B,

489   inactivation of *ERf* proteins results in nucleosomal chromatin structure alterations and decreased

490   abundance of SWI3B and its phosphorylated form in Arabidopsis, and there is an intriguing

491   interdependence between the control of the SWI3B level and DELLA protein accumulation,

492   therefore we examined if ER and the SWI3B participate in transcriptional control of the *GID1*

493   genes previously reported as targets for DELLA (Rosa et al., 2015). The ChIP analysis on *GID1*

494   promoters was performed using nuclei purified from 3-week-old seedlings expressing the ER-

495   GFP and the SWI3B-HIS-STREP-HA proteins.

496   The binding of ER-GFP was detected around -130bp upstream of the TSS in the *GID1a*

497   promoter region while SWI3B bound around the TSS of the *GID1a* promoter (Figure 6A). The

498   ER protein was targeted to two regions around -150bp and -350bp from the TSS in the *GID1b*

499   promoter, SWI3B was localized only -350bp upstream TSS (Figure 6B). ER and SWI3B were

500   similarly cross-linked to the -100bp region of the *GID1c* promoter, but SWI3B was also mapped

501   further upstream to -800bp (Figure 6C).

502

Figure 6. ERf proteins enter the nucleus where ERECTA protein binds the *GID1* promoters similarly to the SWI3B subunit of SWI/SNF CRC (See also Figures S16 and S17). A, ERECTA protein binds to promoter regions of the *GID1a* gene in a region targeted by the SWI/SNF complex in three-week-old plants. (error bars refer to SD, P < 0.05, Student's *t*-test, three biological and technical replicates were performed). B, ERECTA and SWI3B core subunit of SWI/SNF CRCs target promoter regions of *GID1b* gene in three-weeks old plants (error bars refer to SD, P < 0.05, Student's *t*-test, three biological and technical replicates were performed). C, SWI3B binds to the promoter region of the *GID1c* gene in two different regions. One of them is targeted by ERECTA protein in three-week-old plants. D, ERECTA protein binds to promoter regions of the *GID1a* gene in a region targeted by the SWI/SNF complex in five-week-old plants. (error bars refer to SD, P < 0.05, Student's *t*-test, three biological and technical replicates were performed). E, ERECTA targets promoter region of *GID1b* gene in five-week-old plants (error bars refer to SD, P < 0.05, Student's *t*-test, three biological and technical replicates were performed). F, ERECTA binds to the promoter region of the *GID1c* gene in three-week-old plants. The bottom panel in D-F: the binding of native SWI3B protein to its target sites in *GID1a-c* promoter regions is abolished in 5-week-old *er/erl1/erl2* triple mutant plants. G, A model describing the non-canonical nuclear function of ERf proteins in the GA signaling pathway.

521

522 Inspection of ER and SWI3B binding to the *GID1a-c* promoter regions in 5-week-old

523 WT, ER-GFP, and the *er/erl1/erl2* mutant demonstrated that ER binds the same *GID1* promoter

524 regions as in the case of 3-week-old plants (Figure 6 D-F). The SWI3B binding to the promoter

525 of *GID1* genes was abolished by the inactivation of ERf proteins in *er/erl1/erl2* plants. The

526 inactivation of *ER, ERL1,* or *ERL2* did not affect the binding of SWI3B to *GID1a-c* promoter

527 regions in single *er105, erl1,* and *erl2* mutant lines (Supplemental Figure 16). Our study provides

528 evidence that the three ERf proteins have redundant functions regarding proper SWI3B

529 recruitment since only the simultaneous absence of all ERfs proteins abolished SWI3B binding to

530 the *GID1a-c* promoters.

531 Of note, we found a similar binding of HER2 (EGFR-family) receptor and BAF155

532 subunit of SWI/SNF CRCs to the promoter regions of human *BRCA1* and *FBP1* genes

533 (Supplemental Figure 17), indicating that the phenomenon observed for ER may be a general

534 mechanism controlling gene expression that is maintained between kingdoms.

535

536 **Discussion**

537   Inactivation of ERf LRR-RLK family members results in various defects in Arabidopsis

538 growth and development. While it is well established that ERf proteins play distinct roles in the

539 control of epidermal patterning, stomatal development, meristem size, inflorescence architecture,

540 and hormonal signaling, the exact mechanisms underlying the regulatory functions of ERf

541 proteins in these processes are largely unknown (*e.g.,* Chen and Shpak, 2014; Chen et al., 2013b;

542 Qi et al., 2004; Van Zanten et al., 2010; Kosentka et al., 2019).

543   Here we show that the inactivation of Arabidopsis ERf proteins has a broad effect on

544 various regulatory processes, including hormonal signaling, and suggest that these sum responses

545 underlie the severe developmental defects exhibited by the *er/erl1/erl2* mutant. We demonstrate

546 that parallel inactivation of all *ERf* proteins results in severe deregulation of the GA signaling

547 pathway as evidenced by the impairment of GA perception and GA biosynthesis. When taken

548 together, these findings, alongside the identification of NLS and NES sequences in ERf proteins

549 and our demonstration of their translocation into the nucleus, suggest a novel, non-canonical

550 function of ERf proteins (Figure 6G).

551   Our study also reveals an analogy of this system to the previously described XA21 LRR

552 immune receptor in rice (Park and Ronald, 2012) and to the non-canonical signaling mode of the

553 human Epidermal Growth Factor Receptor (EGFR) family (Lee et al., 2015a). Although it should

554 be stressed that these two classes of plant and animal epidermal receptors carry completely

555 unrelated sequences from one another and from the system we describe here (Supplemental Table

556 3), suggesting that the translocation of the membrane receptors to the nucleus may be a general

557 paradigm maintained between plant and animal kingdoms. In addition to their canonical

558 membrane receptor functions, holoreceptor and truncated forms of EGFRs are imported into

559 nuclei *via* ER-mediated retrograde transport, although some of them lack known NLSs (Chen and

560 Hung, 2015).

561   In the nucleus, the EGFR receptors can bind to DNA, interact with various transcription

562 factors. Thereby, nuclear forms of EGFRs are implicated in the control of cell proliferation, DNA

563 replication and repair, and transcription (Chen and Hung, 2015), so their functions extend far

564 beyond the regulation of epidermal patterning.

565   We found here that the Arabidopsis ERECTA LRR-RLK receptor similarly translocates

566 from the plasma membrane into the nucleus. Both intact and N-terminally truncated forms of

567   ERECTA were detectable in the nucleus. A truncated ERECTA carrying only the kinase domain

568   localizes exclusively in the nucleus and partially complements the leaf developmental defects

569   caused by the *er-105* mutation implying a ligand-independent non-canonical signaling function of

570   the ERECTA kinase domain.

571   Furthermore, our data show that the ERf proteins interact through their kinase domains

572   with the SWI3B, and ER can phosphorylate the SWI3B core subunit of the SWI/SNF CRC.

573   SWI/SNF plays a pivotal role in the hormonal crosstalk regulation in both humans and plants

574   (Sarnowska et al., 2016). Moreover, we show that analogously as ER protein, the HER2 member

575   of the EGFR family directly interacts with the BAF155 subunit of human SWI/SNF and co-

576   localizes with BAF155 on some gene promoters providing evidences that such system is likely

577   maintained between kingdoms.

578   Parallel inactivation of all ERf proteins results in alterations of genome-wide nucleosomal

579   chromatin structure and altered transcriptional activity of a large number of genes. The binding of

580   SWI3B to its target regions in the *GID1a-c* promoters is retained in *er-105, erl1,* and *erl2* single

581   mutant lines. By contrast, the *er/erl1/erl2* mutant plants exhibited a reduction in phosphorylation

582   SWI3B protein level and abolished proper SWI3B binding to *GID1* promoter regions together

583   with decreased expression of *GID1a-c* genes, indicating a strong and direct effect of the ERf

584   signaling pathway on SWI/SNF-dependent chromatin remodeling. The *er/erl1/erl2* mutant plants

585   are characterized by a decreased level of endogenous gibberellins; however, they do not

586   accumulate DELLA proteins, similar to the SWI/SNF mutants. Thus, we have demonstrated that

587   the *er/erl1/erl2* mutant plants exhibit severe deregulation of the gibberellin signaling pathway

588   and SWI/SNF-dependent chromatin remodeling. This is, in turn, an attractive explanation of the

589   observed insensitivity of *er/erl1/erl2* mutant to the application of exogenous gibberellin. DELLA

590   proteins are involved in the sequestration of various transcription factors and chromatin

591   remodeling complexes (Phokas and Coates, 2021). In this study, we extend the existing

592   knowledge on DELLA functioning by providing evidence for the existence of the DELLA-

593   SWI3B regulatory module and explaining why some GA-deficient mutant lines with impaired

594   SWI/SNF chromatin remodeling complex do not accumulate DELLA proteins (Figure 5G).

595   Collectively our finding that plant ERf proteins play an important, non-canonical nuclear

596   function, *i.e.,* bind directly to chromatin and control the proper recruitment of SWI/SNF CRCs,

597   which are strongly involved in controlling regulatory processes including hormonal crosstalk

28

598   (Sarnowska et al., 2016), may be a general paradigm for other classes of plant and mammalian

599   membrane receptor kinases.

600

Methods

Plant Material and Growth Conditions

The *Arabidopsis thaliana* ecotype Columbia was used as wild type (WT) in all experiments. The following Arabidopsis mutants were used for analysis: *er-105*, *er-105/swi3b-3* (Sáez et al., 2008), *er/erl1/erl2* plants (Shpak et al., 2004) and *erf* lines in various combinations (Torii et al., 1996), the 35S::GFP Arabidopsis line has been obtained from NASC (N67775). Seeds were sown on soil or plated on ½ Murashige and Skoog medium (Sigma-Aldrich) containing 0.5% sucrose and 0.8% agar. Plants were grown under long day (LD) condition (12h Day/12h Night or 16h Day/8h Night). For GA response tests, plants were sprayed twice a week with 100 μM GA_{4+7} or water (control) for a fast response the 2h of GA_{4+7} treatment was performed.

Construction of Transgenic Lines

Genomic sequences of *ERECTA*, cDNAs of *ERECTA* kinase domain and truncated ERECTA lacking kinase domain (ERΔK) were cloned into binary vector p35S::GW::GFP (F. Turck, Max-Planck-Institut für Züchtungsforschung, in the case of ERECTA), and into pEarley Gate 101 (in the case of the ER kinase domain and ΔKDER; (Earley et al., 2006). Plants were transformed using *Agrobacterium tumefaciens* GV3101 (pMP90) by floral-dip method (Davis et al., 2009). The STOP codon of the *SWI3B* genomic sequence was replaced with HIS-STREP-HA using the recombineering method (Bitrián et al., 2011), moved into pCB1 vector (Heidstra et al., 2004), and transformed into *swi3b-2* Arabidopsis mutant line.

RNA Extraction and qRT-PCR Analysis

Total RNA was isolated from adult (5-week-old) plants using an RNeasy plant kit (Qiagen), treated with a TURBO DNA-free kit (Ambion). Total RNA (2.5μg) was reverse transcribed using a first-strand cDNA synthesis kit (Roche). qRT-PCR assays were performed with SYBR Green Master mix (Bio-Rad) and specific primers for PCR amplification. Housekeeping genes *PP2A* and *UBQ5* (AT1G13320 and AT3G62250, respectively) were used as controls. The relative transcript level of each gene was determined by the $2^{-\Delta\Delta Ct}$ method (Schmittgen and Livak, 2008). Each experiment was performed using at least three independent biological replicates. qRT-PCR primers are listed in Supplemental Dataset 3.

Transcript Profiling and Gene Ontology Analysis

631   RNA was isolated from adult (5-week-old) WT and *er/erl1/erl2* plants using a Plant

632   RNeasy kit (Qiagen) according to the manufacturer's protocol. Transcriptomes were analyzed

633   using 150ng of total RNA as starting material. Targets were prepared with a cDNA synthesis kit

634   followed by biotin labeling with the IVT labeling kit (GeneChip 39IVT Express; Affymetrix) and

635   hybridized to the ATH1 gene chip for 16h as recommended by the supplier. The raw data were

636   analyzed using GenespringGX according to the manual (guided workflow). GO-TermFinder was

637   used for GO analyses of selected groups of genes (Boyle et al., 2004).

638   **Nuclear Fractionation**

639   Nuclei were isolated from 2g of leaves of 3-weeks old Arabidopsis seedlings according to

640   the method previously described by Gaudino and Pikaard (1997). Subsequent nuclear

641   fractionation was performed using the high-salt method, with modifications (Sarnowski et al.,

642   2002).

643   **Protein Interaction Study, Confocal Imaging, Subcellular Localization, Brefeldin A and**

644   **Leptomycin B Treatment, DAPI Staining**

645   Protein interaction was analyzed by performing the immunoprecipitation of ER-GFP or

646   KDER-YFP-HA from nuclei from 4 g of Arabidopsis plants (Saleh et al., 2008). The nuclear

647   extracts were incubated with 25 µL of GFP Magnetic Trap beads (Chromotek) according to

648   manufactures instructions. The presence of SWI3B protein was determined by western blot

649   analysis using anti-SWI3B antibody (Sarnowski et al., 2002).

650   The interaction between human proteins was analyzed by immunoprecipitation of HER2

651   and BAF155 from viscolase treated nuclear extracts prepared, according to Jancewicz et al. 2021.

652   The presence of HER2 and BAF155 was determined by Western blot analysis using anti HER2

653   (CST, 12760) and anti BAF155 (CST, 11956) antibodies.

654   To obtain YFN-ERL1, YFC-ERL1, YFC-ERL2, and YFC-KDER fusions for BiFC (Hu et

655   al., 2002) analysis, cDNAs encoding ERL1 and ERL2 proteins and ERECTA, ERL1, and ERL2

656   C-terminal kinase domains were PCR amplified and cloned into the binary vectors pYFN43 or

657   pYFC43 (Belda-Palazón et al., 2012). The *in vivo* interactions between proteins were detected by

658   BiFC using Leica TCS SP2 AOBS, a laser scanning confocal microscope (Leica Microsystems).

659   Tobacco (*Nicotiana benthamiana*) epidermal cells were infiltrated using *Agrobacterium*

660   *tumefaciens* GV3101 (pMP90) carrying plasmids encoding ERL1, ERL2, or KDER fusions and

661   the p19 helper vector and analyzed by confocal microscopy 3 d later. YFN-RFP and YFC-RFP

662 fusions were used to detect transformed cells in the BiFC assays (Sarnowska et al., 2013); at least

663 five nuclei were analyzed in three separate experiments.

664 The vesicle trafficking inhibitor BFA (Sigma Aldrich) was used at the 25µM

665 concentration at the following time points 40 min, 90 min, and 120 min. The NES-dependent

666 nuclear export inhibitor Leptomycin B was used at the 200 nM concentration 4h before

667 microscopy observation. Nuclei were stained with 4',6-diamidino-2-phenylinodole (DAPI) at the

668 1µg/mL concentration for 30 min. The observation was carried out on the root tip of about two

669 weeks old plants incubated directly before in ½ MS alone or with the addition of proper

670 compound (BFA or Leptomycin B, respectively). Every time 30 min before the end of

671 incubation, DAPI was added.

Chromatin Immunoprecipitation

673 ChIP experiments were performed as described previously (Sacharowski et al., 2015) on

674 three or five-week-old WT, ER-GFP, SWI3B-His-Strep-HA, and *er/erl1/erl2* plants cross-linked

675 under vacuum using formaldehyde (final concentration: 1%) and Bis-(sulfosuccinimidyl)

676 glutarate (final concentration: 1mM). For ER-GFP, chromatin immunoprecipitation was

677 performed with GFP-Trap M (Chromotek). For SWI3B ChIP experiments, NiNTA Agarose

678 (Qiagen) or, in the case of anti-SWI3B antibody, the magnetic protein A and G dynabeads

679 (Dynal) were used. ChIP enrichment was determined using qPCR, and relative fold change was

680 calculated using the $2^{-\Delta\Delta Ct}$ method (Schmittgen and Livak, 2008). The TA3 retrotransposon was

681 used as negative control (Pastore et al., 2011). Primers used in ChIP experiments are listed in

682 Supplemental Dataset 3.

683 Chromatin from the SKBR-3 human cell line was immunoprecipitated according to

684 (Komata et al., 2014 and Jancewicz et al., 2021). Recovered chromatin was incubated O/N at 4°C

685 with the following antibodies: anti BAF155 (CST, 11956), antiHER2 (CST, 12760), and Normal

686 Rabbit IgG (CST, 2729, mock control). Results were calculated based on the $2^{-\Delta\Delta Ct}$ (Schmittgen

687 and Livak, 2008). The relative fold enrichment of the analyzed sample represents the fold change

688 with reference to IgG (mock) sample. A set of primers used for ChIP-qPCR analysis is listed in

689 Supplementary Dataset 3.

MNase Mapping of Genome-wide Nucleosome Positioning and MNase-qPCR

691   The nuclear extraction, MNase treatment, subsequent NGS analyses, and confirmatory

692   MNase-qPCR were performed according to (Sacharowski et al., 2015) on 5 week old plant

693   material.

694   **Gibberellin Analysis**

695   About 200 mg of frozen materials from 5 week old plants were used to extract and purify the GA

696   as described in Plackett et al. (2012) with minor modifications. GA was quantified using MS/MS

697   analysis using 4000 Triple Quad (AB Sciex Germany GmbH, Darmstadt, Germany) in multiple

698   reaction monitoring (MRM) scan with electrospray ionization (ESI) as described in Salem et al.,

699   (2016). The mass spectrometry attached to UPLC system (e.g., Waters Acquity UPLC system,

700   Waters, Machester, UK) separation was achieved on a reversed phase C18-column (100 mm ×

701   2.1 mm 1.8 μm).

702   ***In vitro* Phosphorylation Analysis and *in vivo* Kinase Assay**

703   SWI3B-6xHis was overexpressed and purified, according to Sarnowski et al. (2002). The

704   KDER (pDEST-6xHis-MBP vector) was purified using tandem purification using MBP and Ni-

705   NTA resins. *In vitro* kinase assay was performed according to the method described by (Allen et

706   al., 2007). Phosphorylation was detected by Western blot analysis using an anti-Thiophosphate

707   ester antibody (ab92570; Abcam) and by the MS/MS analysis.

708   *In vivo* phosphorylation analysis was performed using a 2D western blot assay on nuclear

709   extracts from 5 weeks old WT and *er/erl1/erl2* plants (Saleh et al., 2008). For isoelectrofocusing

710   (IEF), nuclear proteins were prepared according to Kubala et al. (2015). The IEF was performed

711   on the 7cm length gel strips with immobilized pH gradients 3-10 and 3-6 (BioRad). After IEF,

712   the equilibration of immobilized pH gradient was performed according to Wojtyla et al. (2013).

713   The SWI3B protein was detected by Western blotting using an anti SWI3B antibody (Sarnowski

714   et al., 2002). The *in vivo* phosphorylation was identified based on the changes of SWI3B

715   isoelectric point (*pI*) (Mayer et al., 2015).

716   **Accession Numbers**

717   Microarray and MNase-seq data are available in the ArrayExpress database

718   (www.ebi.ac.uk/arrayexpress) under E-MTAB-5595 and E-MTAB-5830 accession numbers,

719   respectively.

720

721 **Supplemental Data**

722
723

724 **Supplemental Figure 1.** Comparative analysis of genes with altered expression in *er/erl1/erl2*

725 and *ga1-3* mutants. A, Combinations of *erf* mutants have distinct effects on height of Arabidopsis

726 plants. Error bars refer to SD,* = P < 0.05, Student's t test. B, Genes showing altered expression

727 in the *er/erl1/erl2* mutant plants. C, Venn diagrams indicating genes contrastingly up-regulated in

728 *er/erl1/erl2* and down-regulated in *ga1-3* plants. D, Venn diagrams indicating genes contrastingly

729 down-regulated in *er/erl1/erl2* and up-regulated in *ga1-3* plants. E, ERf proteins control the

730 expression of genes down-regulated in *ga1-3,* which are either DELLA repressed or DELLA

731 independent. F, ERf proteins control the expression of genes up-regulated in *ga1-3,* which are

732 either DELLA activated or DELLA independent.

733

734 **Supplemental Figure 2.** The *er/erl1/erl2* mutant displays severely impaired response to

735 exogenous GA treatment and slightly enhance *ga1-3* phenotypic traits. A, The 14 days old

736 *er/erl1/erl2* plants treated with GA_{4+7} did not show rosette expansion indicating defects in GA

737 response. Error bars refer to SD,* =P < 0.05, Student's t test, n= 30 plants. B, Two-month-old

738 GA_{4+7} treated *er/erl1/erl2* plants show accelerated flowering compared to mock treated control.

739 Scale bar= 1cm. n= 30 plants. C, Two-months old *er/erl1/erl2* plants. Scale bar= 1cm. n= 30

740 plants. D, Three-weeks old *ga1-3* plants crossed with *erf* mutants in various combinations show

741 mostly the phenotypic traits characteristic for *ga1-3*. Scale bar= 1 cm. E, The phenotypic traits of

742 5-weeks old plants carrying *erf* mutations crossed with *ga1-3* in various combinations grown in

743 long day conditions. Scale bar= 1 cm.

744

745 **Supplemental Figure 3.** *er/erl1/erl2* plants exhibit deficiency in gibberellin intermediates.

746 Left panel: *er/erl1/erl2* mutant exhibits dramatically reduced level of GA_{12} and GA_{24} gibberellin

747 intermediates (error bars-SD, P < 0.05, Student's *t*-test, three biological and technical replicates

748 were assayed). Right panel: schematic representation of alteration in GA biosynthesis pathway in

749 *er/erl1/erl2* plants.

750

751 **Supplemental Figure 4.** 35S::ERECTA-GFP construct complements the *er-105* mutation.

752

Supplemental Figure 5. ERECTA protein is detected in various cell compartments including endosomes and accumulate in the nuclei periphery after BFA treatment. A, In cell pairs of stomata, ERECTA-GFP was detected in circles around the positions of nuclei. Scale bar=10µm. B, Accumulation of ERECTA protein in the BFA bodies after Brefeldin A treatment. Note the enhanced presence of BFA bodies after 40 min (mid column) and 90 min (right column) BFA treatment. Scale bar=10µm.

Supplemental Figure 6. The ERL1 and ERL2 proteins carry defined NLS in their kinase domains. A, The NLS prediction in the kinase domain of ERL1 and ERL2 proteins has been done using cNLS mapper (Kosugi et al., 2009a; Kosugi et al., 2009b). NLS score in range 5-7 means that protein is partially localized in the nucleus and cytoplasm. Bottom panel: The alignment of ERECTA, ERL1, and ERL2 protein sequences (part of kinase domains carrying NLS) using PRALINE indicates high amino-acid sequence conservation between analyzed proteins. Consistency is determined within range 1-10, where 1 means least conserved substitution and 10-the most conserved substitution (Simossis et al., 2005). B, Western blot analysis with anti-GFP antibody confirms nuclear localization of ERECTA protein which undergoes proteolytic processing. The samples were standardized by western blotting with anti H3 antibody. C, Schematic presentation of full length and deletion variants of ERECTA protein used for the localization study. ER – ERECTA protein with complete amino acids sequence; ΔKDER – truncated ERECTA protein lacking kinase domain; KDER – the kinase domain of ERECTA protein.

Supplemental Figure 7. The kinase domain of ERECTA (KDER) has ability to complement the *er-105* leaf phenotypic traits. A, Rosette leaves of WT (upper), *er-105* (mid), and *er-105/*KDER-YFP (lower panel). Graphical alignment of corresponding leaves indicating partial complementation of *er* phenotypic traits by KDER. Scale bar= 1cm. B, Cauline leaves of WT (upper), *er-105* (mid), and *er-105/*KDER-YFP (lower panel). Graphical alignment of corresponding laves indicating partial complementation of *er* phenotypic traits by KDER. Scale bar= 1cm. C, The kinase domain of ERECTA cannot restore all (i.e., stem elongation) phenotypic traits of the *er-105* mutant line. Scale bar= 1cm.

784 **Supplemental Figure 8.** ERECTA protein enters to the nucleus and localizes in various sub-
785 nuclear fractions.

786

787 **Supplemental Figure 9.** Negative controls for bimolecular fluorescence complementation assay.
788 Negative controls for BiFC interaction analysis of ER, ERL1, ERL2 kinase domains fused to
789 YFC and SWI3B fused to YFN, including the RFP channel. Scale bar 10 μm.

790

791 **Supplemental Figure 10.** Human SWI3-type BAF155 co-precipitates with HER2 EGFR family
792 membrane receptor from human cells nuclei.

793

794 **Supplemental Figure 11.** *er/elr1/erl2* mutant plants show affected chromatin organization
795 demonstrated as altered chromocenters number.
796 Upper panel: exemplary pictures of WT and *er/erl1/erl2* nuclei.
797 Lower panel: calculation of chromocenters (n=20 nuclei for each genotype).

798

799 **Supplemental Figure 12.** ERf proteins inactivation has a severe impact on genome-wide
800 nucleosome positioning. A, Nucleosome changes identified in the *er/erl1/erl2* triple mutant
801 plants. B, Genome-wide nucleosome distribution patterns surrounding the transcription start site
802 (TSS). C, Nucleosome distribution patterns surrounding the TSS of GA-related genes showing
803 altered expression in the *er/erl1/erl2* triple mutant plants. D, The alteration of nucleosomal
804 structure on *PRE1*, *GID1a,* and *GID1b loci* misexpressed in the *er/erl1/erl2* triple mutant plants
805 and targeted by the SWI/SNF CRC. Red boxes indicate nucleosome alterations. E, Confirmatory
806 MNase-qPCR for selected genes with altered nucleosomes.

807

808 **Supplemental Figure 13.** Kinase domain of ERECTA phosphorylates SWI3B protein. A,
809 Western blot with anti His6 antibody for detection of MBP-His6-KDER and His6-SWI3B
810 proteins purified from bacteria. B, Western blot with anti-Thiophosphate ester antibody
811 indicating no phosphorylation of SWI3B protein in the absence of KDER (negative control). C,
812 Western blot with anti-Thiophosphate ester antibody (ab92570; Abcam) showing
813 autophosphorylation of KDER in the absence of SWI3B protein. D, Identification of active
814 phosphorylation sites in KDER by MS/MS analysis. E, Identification of active phosphorylation

815   sites in SWI3B by MS/MS analysis. F, KDER phosphorylates SWI3B at the SWIRM and SANT

816   domains.

817

818   **Supplemental Figure 14.** GA-deficient mutant lines with inactivated subunits of SWI/SNF

819   complexes do not accumulate RGA DELLA protein. A, GA-deficient *swi3c* plants are unable to

820   over accumulate RGA protein. B, GA-deficient *brm* plants are unable to over accumulate RGA

821   protein.

822

823   **Supplemental Figure 15.** Negative controls for bimolecular fluorescence complementation

824   assay.

825   Negative controls for BiFC interaction analysis of SWI3B, RGA, and RGL1 fused to YFC, and

826   SWI3B fused to YFN, including the RFP channel. Scale bar 10 μm.

827

828   **Supplemental Figure 16.** Proper SWI3B binding to *GID1a-c* promoter regions is abolished in

829   the *er/erl1/erl2* whereas occurs in single *er-105, erl1* or *erl2* mutant lines. A, SWI3B targets

830   promoter region of *GID1a* gene in five-weeks old plants WT, *er-105, erl1* or *erl2* but is abolished

831   in triple *er/erl1/erl2* mutant plants (error bars refer to SD, P < 0.05, Student's t test, three

832   biological and technical replicates were used). B, SWI3B targets promoter region of *GID1b* gene

833   in five-weeks old plants WT, *er-105, erl1* or *erl2* but is abolished in triple *er/erl1/erl2* mutant

834   plants (error bars refer to SD, P < 0.05, Student's t test, three biological and technical replicates

835   were used). C, SWI3B targets promoter region of *GID1c* gene in five-weeks old plants WT, *er-

836   105, erl1* or *erl2* but is abolished in triple *er/erl1/erl2* mutant plants (error bars refer to SD, P <

837   0.05, Student's t test, three biological and technical replicates were used).

838

839   **Supplemental Figure 17.** Human SWI3-type BAF155 targets together with HER2 EGFR family

840   membrane receptor *FBP1* and *BRCA1* genes *loci*. A, BAF155 subunit of human SWI/SNF

841   complex binds *Fructose-1,6-Bisphosphatase locus* together with HER2 member of EGFR

842   membrane receptor family. B, BAF155 subunit of human SWI/SNF complex binds *BRCA1 locus*

843   together with HER2 member of EGFR membrane receptor family.

844

845   **Supplemental Table 1.** Genes classified to "Response to Gibberellin" GO term and showing

846   down-regulated expression level in the *er/erl1/erl2* mutant.

847

848   **Supplemental Table 2.** Genes with up-regulated expression in *er/erl1/erl2* mutant plants

849   classified to GO-terms of leaf epidermal and stomatal cell differentiation.

850

851   **Supplemental Table 3.** Functional analogies between arabidopsis ERf proteins and the human

852   EGFR membrane receptors.

853

854   **Supplemental dataset 1.** Comparative analysis of transcript profiling and MNase-seq data.

855   **Sub-table 1.** Transcript profiling using ATH1 microarray analysis to identify genes down-
856   regulated in *er/erl1/erl2* mutant line.

857   **Sub-table 2.** Transcript profiling using ATH1 microarray analysis to identify genes up-regulated
858   in *er/erl1/erl2* mutant line.
859   **Sub- table 3.** GO analysis of genes down-regulated in *er/erl1/erl2* mutant line.

860   **Sub- table 4.** GO analysis of genes up-regulated in *er/erl1/erl2* mutant line.
861   **Sub-table 5.** Comparative transcript profiling analysis for genes down-regulated in *er/erl1/erl2*
862   and *ga1-3* mutants lines.

863   **Sub-table 6.** GO analysis of *er/erl1/erl2* and *ga1-3* down-regulated genes.

864   **Sub-table 7.** Comparative transcript profiling analysis for genes up-regulated in *er/erl1/erl2* and
865   *ga1-3* mutants lines.
866   **Sub-table 8.** GO analysis of genes up-regulated in *ga1-3* and *er/erl1/erl2*.
867   **Sub-table 9.** Genes with altered nucleosome positioning in promoter region -3000 to TSS.

868   **Sub-table 10.** GO analysis of genes with altered nucleosome positioning identified in promoter
869   region -3000 to TSS.

870   **Sub-table 11.** Genes with altered nucleosome positioning identified in promoter region -3000 to
871   TSS and down-regulated in *er/erl1/erl2* microarray.

872   **Sub-table 12.** Genes with altered nucleosome positioning identified in promoter region -3000 to
873   TSS and up-regulated in *er/erl1/erl2* microarray.
874   **Sub-table 13.** GO analysis for genes with altered nucleosome positioning identified in promoter
875   region -3000 to TSS and down-regulated in *er/erl1/erl2* microarray.

876   **Sub-table 14.** GO analysis for genes with altered nucleosome positioning identified in promoter
877   region -3000 to TSS and up-regulated in *er/erl1/erl2* microarray.
878

879   **Supplemental dataset 2.** Comparison of ER, ERL1, and ERL2 protein sequences with
880   highlighted important domains including NLS.

881   ClustalW was used to align ER, ERL1, and ERL2 sequences. Under conserved amino acid is

882   asterisk mark, highly similar or similar amino-acids are marked :: and . respectively. LRR domain

883   is marked as gray background, amino-acids crucial for EPFs or TMM interaction are indicated

884   with bold. Transmembrane domain, juxtamembrane domain, and kinase domain are indicated

885   with bold green, orange, and blue color fonts, respectively (Kosentka et al., 2017). The predicted

886   NLS sequence is marked in a dotted line frame (Kosugi et al., 2009b).

887

888   **Supplemental Dataset 3.** Primers used in this work.

889   **Supplemental Movie 1. The ERECTA protein undergoes endocytosis.**

890   **Supplemental Movie 2. The ERECTA protein undergoes endocytosis.**

891

900 **FIGURE LEGENDS**

901 **Figure 1.** *ERf* inactivation affects Arabidopsis development, causes transcriptomic changes

902 overlapping with the effect of *ga1-3* mutation and impairs GA biosynthesis and signaling (See

903 also Figures S1, S2 and S3). A, Phenotypic changes conferred by combinations of *erf* mutations.

904 Scale bar= 1 cm. B, Overlapping down-regulated genes in *er/erl1/erl2* and *ga1-3* plants. C,

905 Overlapping up-regulated genes in *er/erl1/erl2* and *ga1-3* plants. D, The *er/erl1/erl2* plants

906 exhibit impaired GA response. 14- days old LD (12h day/12 night) grown WT and *er/erl1/erl2*,

907 sprayed twice a week with water (upper row) or 100µM GA_{4+7} (lower row). Arrows-*er/erl1/erl2*

908 plants. Scale bar= 1cm. E, The GA response is retained to various levels in combinations of *erf*

909 mutants. Error bars-SD,* =P < 0.05, Student's *t*-test, *n*= 30 plants. F, The response of various *erf*

910 mutants to 1µM Paclobutrazol treatment. Error bars-SD,* =P < 0.05, Student's t test, n= 30

911 plants. G, The *er/erl1/erl2* mutant exhibits altered transcription of *GID1* GA receptor genes (error

912 bars-SD, P < 0.05, Student's *t*-test, three biological and technical replicates were assayed). H,

913 The *er/erl1/erl2* mutant displays altered GA biosynthesis and metabolism-related genes

914 expression (error bars-SD, P < 0.05, Student's *t*-test, three biological and technical replicates

915 were assayed). I, The *er/erl1/erl2* mutant exhibits dramatically reduced level of bioactive GA_{4+7}

916 gibberellin (error bars-SD, P < 0.05, Student's *t*-test, three biological and technical replicates

917 were assayed). J, The *er/erl1/erl2* mutant shows decreased level of the DELLA protein RGA.

918

919 **Figure 2.** Subcellular localization of ERECTA protein (See also Figures S4 and S5). A,

920 ERECTA is localized in plasma-membrane and endosomes in epidermal cells of 7-days old

921 seedlings. ER-GFP, or free GFP visualized using GFP channel. FM4-64 specifically stains

922 plasma-membranes. Scale bar=10µm. B, Root-tip images of approximately two-week-old (14-17

923 days) ER-GFP seedlings showing nuclear localization of ERECTA protein at considerable

924 frequency. C, Root-tip images of 12-day-old ER-GFP seedlings serving as the control for D and

925 E. D, Brefeldin A treatment enhanced the localization of ERECTA protein in Brefeldin A (BFA)

926 bodies. Roots of 12-day-old Arabidopsis seedlings. E, Leptomycin B treatment enhanced the

927 nuclear localization of ERECTA Free GFP was used as a control in C, D, and E, cell nuclei were

928 stained with DAPI, scale bar= 50µm. F, Letomycin B enhances nuclear presence of ER protein.

929 The GFP/DAPI ratio calculated per area for roots of plants expressing ER-GFP protein.

930

931 **Figure 3.** Nuclear function of ERf proteins (See also Figures S6, S7, S8, S9, and S10). A, Root-

932 tip images of approximately two-week-old (14-17 days) plants expressing ER-GFP, KDER-YFP-

933 HA (the kinase domain of the ER protein), ERΔK-YFPHA (truncated ER protein lacking the

934 kinase domain) proteins indicating that the kinase domain is necessary for the nuclear localization

935 of ER protein. WT and GFP expressing plants-negative controls. Panel 2 in the ER-GFP indicates

936 nuclear localization of ER protein appearing at considerable frequency. Cell nuclei were stained

937 with DAPI. Scale bar=25 µm. B, The *er-105/swi3b3* double mutant shows more retarded growth

938 than either *er-105* or *swi3b3* plants. Scale bar= 1cm. C, The *er/erl1/erl2* triple mutant exhibits

939 reduced SWI3B protein level. D, ER-GFP or free GFP (negative control) pull-down from the

940 nucleus and anti-SWI3B western blotting indicate a specific ER-SWI3B interaction. E,

941 Immunoprecipitation of KDER-YFP-HA from the nucleus indicated that the kinase domain of

942 ER interacts with SWI3B. F, ER, ERL1, and ERL2 kinase domains interact with SWI3B in the

943 nucleus. Bimolecular Fluorescence Complementation assay (BiFC) in epidermis of tobacco

944 leaves. Scale bar = 10µm.

945

946 **Figure 4.** ER and *SWI3B* interact genetically and affect both GA biosynthesis and response

947 pathways (See also Figures S11 and S12). A, The *er-105/swi3b-3* double mutant exhibits more

948 retarded growth than the *er-105* and *swi3b-3* (three-weeks old plants). Graphical alignment of

949 corresponding leaves. Scale bar= 1 cm. B, The hypersensitivity of 1-week-old *swi3b-3* hypocotyl

950 to GA treatment is abolished by introducing *er-105*. C, Roots of all tested 1-week-old genotypes

951 similarly respond to PAC treatment (error bars-SD, $*P < 0.01$,$** P < 0.001$, $***P<0.0001$,

952 Student's *t*-test). D, Hypocotyls of all tested 1-week-old genotypes similarly respond to PAC

953 treatment, right panel- hypocotyl length comparison for PAC treated plants only (error bars-SD,

954 $*P < 0.01$,$** P < 0.001$, $***P<0.0001$ Student's *t*-test). E, *swi3b-3* weak, point mutant line and

955 *er-105/swi3b-3* exhibit elevated *SWI3B* transcript level, the *SWI3B* expression is elevated after

956 supplementation with bioactive GA_{4+7} in all genotypes except *swi3b-3* (error bars-SD, $P < 0.05$,

957 Student's *t*-test). F, The examination of *GID1* genes indicated that almost all examined lines

958 responded to GA treatment, but the *swi3b-3* line was insensitive for GA-induced transcriptional

959 changes (error bars-SD, $P < 0.05$, Student's *t*-test). G, The examination of GA biosynthesis genes

960 indicated that almost all examined lines responded to GA treatment, but the *swi3b-3* line was

961   insensitive for GA-induced transcriptional changes except *GA20ox2* expression (error bars-SD, P

962   < 0.05, Student's *t*-test).

963

964   **Figure 5.** ERf proteins are responsible for the phosphorylation of SWI3B protein, while DELLA

965   proteins control SWI3B protein abundance (See also Figures S13, S14, and S15). A, Coomassie

966   staining of MBP-His6-KDER and His6-SWI3B proteins purified from bacteria. B, Western blot

967   with anti-Thiophosphate ester antibody (ab92570; Abcam) showing *in vitro* SWI3B

968   phosphorylation by KDER. C, 2D Western blot assay with anti SWI3B antibody indicating *in*

969   *vivo* phosphorylation alteration of SWI3B protein in *er/erl1/erl2* mutant. D, SWI3B and RGA

970   and RGL1 proteins in the nuclei of living cells. Bimolecular Fluorescence Complementation

971   assay (BiFC) in epidermis of tobacco leaves. Scale bar = 10µm. E, The amounts of SWI3B and

972   RGA proteins in plants are oppositely regulated by PAC treatment. F, The disappearance of

973   SWI3B protein is PAC-dose dependent. G, The PAC-dependent degradation of SWI3B is

974   abolished by the MG132 treatment, a known proteasome inhibitor. H, The *ga1-3* mutant

975   constitutively accumulating DELLA proteins exhibits the decreased level of SWI3B, which is

976   restored to WT levels upon GA treatment. I, The triple DELLA mutant exhibits a WT-like level

977   of SWI3B protein, and the PAC treatment does not influence SWI3B level in this background. J,

978   Schematic model highlighting ERf and DELLA impact on the SWI3B protein.

979

980   **Figure 6.** ERf proteins enter the nucleus where ERECTA protein binds the *GID1* promoters

981   similarly to the SWI3B subunit of SWI/SNF CRC (See also Figures S16 and S17). A, ERECTA

982   protein binds to promoter regions of the *GID1a* gene in a region targeted by the SWI/SNF

983   complex in three-week-old plants. (error bars refer to SD, P < 0.05, Student's *t*-test, three

984   biological and technical replicates were performed). B, ERECTA and SWI3B core subunit of

985   SWI/SNF CRCs target promoter regions of *GID1b* gene in three-weeks old plants (error bars

986   refer to SD, P < 0.05, Student's *t*-test, three biological and technical replicates were performed).

987   C, SWI3B binds to the promoter region of the *GID1c* gene in two different regions. One of them

988   is targeted by ERECTA protein in three-week-old plants. D, ERECTA protein binds to promoter

989   regions of the *GID1a* gene in a region targeted by the SWI/SNF complex in five-week-old plants.

990   (error bars refer to SD, P < 0.05, Student's *t*-test, three biological and technical replicates were

991   performed). E, ERECTA targets promoter region of *GID1b* gene in five-week-old plants (error

992   bars refer to SD, P < 0.05, Student's *t*-test, three biological and technical replicates were

993   performed). F, ERECTA binds to the promoter region of the *GID1c* gene in three-week-old

994   plants. The bottom panel in D-F: the binding of native SWI3B protein to its target sites in *GID1a-*

995   *c* promoter regions is abolished in 5-week-old *er/erl1/erl2* triple mutant plants. G, A model

996   describing the non-canonical nuclear function of ERf proteins in the GA signaling pathway.

997

998 **References**

999

1000 **Allen JJ, Li M, Brinkworth CS, Paulson JL, Wang D, Hübner A, Chou W-H, Davis RJ,**

1001 **Burlingame AL, Messing RO, et al** (2007) A semisynthetic epitope for kinase substrates.

1002 Nat Methods 2007 46 **4**: 511–516

1003 **Archacki R, Buszewicz D, Sarnowski TJ, Sarnowska E, Rolicka AT, Tohge T, Fernie AR,**

1004 **Jikumaru Y, Kotlinski M, Iwanicka-Nowicka R, et al** (2013) BRAHMA ATPase of the

1005 SWI/SNF Chromatin Remodeling Complex Acts as a Positive Regulator of Gibberellin-

1006 Mediated Responses in Arabidopsis. PLoS One **8**: e58588

1007 **Archacki R, Yatusevich R, Buszewicz D, Krzyczmonik K, Patryn J, Iwanicka-Nowicka R,**

1008 **Biecek P, Wilczynski B, Koblowska M, Jerzmanowski A, et al** (2016) Arabidopsis

1009 SWI/SNF chromatin remodeling complex binds both promoters and terminators to regulate

1010 gene expression. Nucleic Acids Res **45**: 3116–3129

1011 **Belda-Palazón B, Ruiz L, Martí E, Tárraga S, Tiburcio AF, Culiáñez F, Farràs R, Carrasco**

1012 **P, Ferrando A** (2012) Aminopropyltransferases Involved in Polyamine Biosynthesis

1013 Localize Preferentially in the Nucleus of Plant Cells. PLoS One. doi:

1014 10.1371/journal.pone.0046907

1015 **Bitrián M, Roodbarkelari F, Horváth M, Koncz C** (2011) BAC-recombineering for studying

1016 plant gene regulation: Developmental control and cellular localization of SnRK1 kinase

1017 subunits. Plant J **65**: 829–842

1018 **Bogdan S, Klämbt C** (2001) Epidermal growth factor receptor signaling. Curr Biol **11**: R292–

1019 R295

1020 **Boyle EI, Weng S, Gollub J, Jin H, Botstein D, Cherry JM, Sherlock G** (2004)

1021 GO::TermFinder - Open source software for accessing Gene Ontology information and

1022 finding significantly enriched Gene Ontology terms associated with a list of genes.

1023 Bioinformatics **20**: 3710–3715

1024 **Cai H, Huang Y, Chen F, Liu L, Chai M, Zhang M, Yan M, Aslam M, He Q, Qin Y** (2021)

1025 ERECTA signaling regulates plant immune responses via chromatin-mediated promotion of

1026 WRKY33 binding to target genes. New Phytol **230**: 737–756

1027 **Cai H, Zhao L, Wang L, Zhang M, Su Z, Cheng Y, Zhao H, Qin Y** (2017) ERECTA

1028 signaling controls Arabidopsis inflorescence architecture through chromatin-mediated

activation of PRE1 expression. New Phytol **214**: 1579–1596

Cao D, Cheng H, Wu W, Soo HM, Peng J (2006) Gibberellin mobilizes distinct DELLA-dependent transcriptomes to regulate seed germination and floral development in Arabidopsis. PLANT Physiol **142**: 509–525

Casalini P, Iorio M V., Galmozzi E, Ménard S (2004) Role of HER receptors family in development and differentiation. J Cell Physiol **200**: 343–350

Chen M-K, Wilson RL, Palme K, Ditengou FA, Shpak ED (2013) ERECTA Family Genes Regulate Auxin Transport in the Shoot Apical Meristem and Forming Leaf Primordia. Plant Physiol **162**: 1978–1991

Chen MK, Hung MC (2015) Proteolytic cleavage, trafficking, and functions of nuclear receptor tyrosine kinases. FEBS J **282**: 3693–3721

Chen MK, Shpak ED (2014) ERECTA family genes regulate development of cotyledons during embryogenesis. FEBS Lett **588**: 3912–3917

Chenlong Li, Gu L, Gao Lei, Chen C, Wei CQ, Qiu Q, Chien CW, Wang S, Jiang L, Ai LF, Chen CY, Yang S, Nguyen V, Qi Y, Snyder MP, Burlingame AL, Kohalmi SE, Huang S, Cao X, Wang ZY, Wu K, Chen X CY (2016) Concerted genomic targeting of H3K27 demethylase REF6 and chromatin-remodeling ATPase BRM in Arabidopsis. Nat Genet **48**: 687–693

la Cour T, Kiemer L, Mølgaard A, Gupta R, Skriver K, Brunak S (2004) Analysis and prediction of leucine-rich nuclear export signals. Protein Eng Des Sel **17**: 527–536

Craft N, Shostak Y, Carey M, Sawyers CL (1999) A mechanism for hormone-independent prostate cancer through modulation of androgen receptor signaling by the HER-2/neu tyrosine kinase. Nat Med **5**: 280–5

Davis AM, Hall A, Millar AJ, Darrah C, Davis SJ (2009) Protocol: Streamlined sub-protocols for floral-dip transformation and selection of transformants in Arabidopsis thaliana. Plant Methods **5**: 3

Du J, Jiang H, Sun X, Li Y, Liu Y, Sun M, Fan Z, Cao Q, Feng L, Shang J, et al (2018) Auxin and Gibberellins Are Required for the Receptor-Like Kinase ERECTA Regulated Hypocotyl Elongation in Shade Avoidance in Arabidopsis. Front Plant Sci. doi: 10.3389/fpls.2018.00124

Earley KW, Haag JR, Pontes O, Opper K, Juehne T, Song K, Pikaard CS (2006) Gateway-

1060   compatible vectors for plant functional genomics and proteomics. Plant J. doi:

1061   10.1111/j.1365-313X.2005.02617.x

1062   **Gaudino RJ, Pikaard CS** (1997) Cytokinin induction of RNA polymerase I transcription in

1063   Arabidopsis thaliana. J Biol Chem **272**: 6799–6804

1064   **Giri DK, Ali-Seyed M, Li L-Y, Lee D-F, Ling P, Bartholomeusz G, Wang S-C, Hung M-C**

1065   (2005) Endosomal transport of ErbB-2: mechanism for nuclear entry of the cell surface

1066   receptor. Mol Cell Biol **25**: 11005–11018

1067   **Griffiths J, Murase K, Rieu I, Zentella R, Zhang Z-L, Powers SJ, Gong F, Phillips AL,**

1068   **Hedden P, Sun T, et al** (2006) Genetic characterization and functional analysis of the GID1

1069   gibberellin receptors in Arabidopsis. Plant Cell **18**: 3399–3414

1070   **Haasen D, Köhler C, Neuhaus G, Merkle T** (2002) Nuclear export of proteins in plants:

1071   AtXPO1 is the export receptor for leucine-rich nuclear export signals in Arabidopsis

1072   thaliana. Plant J **20**: 695–705

1073   **Heidstra R, Welch D, Scheres B** (2004) Mosaic analyses using marked activation and deletion

1074   clones dissect Arabidopsis SCARECROW action in asymmetric cell division. Genes Dev

1075   **18**: 1964–1969

1076   **Ho CMK, Paciorek T, Abrash E, Bergmann DC** (2016) Modulators of Stomatal Lineage

1077   Signal Transduction Alter Membrane Contact Sites and Reveal Specialization among

1078   ERECTA Kinases. Dev Cell **38**: 345–357

1079   **Hsu JL, Hung MC** (2016) The role of HER2, EGFR, and other receptor tyrosine kinases in

1080   breast cancer. Cancer Metastasis Rev **35**: 575–588

1081   **Hu CD, Chinenov Y, Kerppola TK** (2002) Visualization of interactions among bZIP and Rel

1082   family proteins in living cells using bimolecular fluorescence complementation. Mol Cell **9**:

1083   789–798

1084   **Hung LY, Tseng JT, Lee YC, Xia W, Wang YN, Wu ML, Chuang YH, Lai CH, Chang WC**

1085   (2008) Nuclear epidermal growth factor receptor (EGFR) interacts with signal transducer

1086   and activator of transcription 5 (STAT5) in activating Aurora-A gene expression. Nucleic

1087   Acids Res **36**: 4337–4351

1088   **James Cao H, Lin H-Y, Luidens MK, Davis FB, Davis PJ** (2009) Cytoplasm-To-Nucleus

1089   Shuttling Of Thyroid Hormone Receptor-β1 (Trβ1) Is Directed From A Plasma Membrane

1090   Integrin Receptor By Thyroid Hormone. Endocr Res **34**: 31–42

1091   **Karachaliou N, Pilotto S, Lazzari C, Bria E, de Marinis F, Rosell R** (2016) Cellular and

1092   molecular biology of small cell lung cancer: an overview. Transl Lung Cancer Res **5**: 2–15

1093   **Komata M, Katou Y, Tanaka H, Nakato R, Shirahige K, Bando M** (2014) Chromatin

1094   immunoprecipitation protocol for mammalian cells. Methods Mol Biol **1164**: 33–38

1095   **Kosentka PZ, Zhang L, Simon YA, Satpathy B, Maradiaga R, Mitoubsi O, Shpak ED**

1096   (2017) Identification of critical functional residues of receptor-like kinase ERECTA. J Exp

1097   Bot **68**: 1507–1518

1098   **Kosugi S, Hasebe M, Matsumura N, Takashima H, Miyamoto-Sato E, Tomita M,**

1099   **Yanagawa H** (2009a) Six classes of nuclear localization signals specific to different binding

1100   grooves of importin alpha. J Biol Chem **284**: 478–485

1101   **Kosugi S, Hasebe M, Tomita M, Yanagawa H** (2009b) Systematic identification of cell cycle-

1102   dependent yeast nucleocytoplasmic shuttling proteins by prediction of composite motifs.

1103   Proc Natl Acad Sci U S A **106**: 10171–10176

1104   **Kubala S, Garnczarska M, Wojtyla Ł, Clippe A, Kosmala A, Zmieńko A, Lutts S, Quinet M**

1105   (2015) Deciphering priming-induced improvement of rapeseed (Brassica napus L.)

1106   germination through an integrated transcriptomic and proteomic approach. Plant Sci **231**:

1107   94–113

1108   **Lee H-H, Wang Y-N, Hung M-C** (2015a) Non-canonical signaling mode of the epidermal

1109   growth factor receptor family. Am J Cancer Res **5**: 2944–2958

1110   **Lee JS, Hnilova M, Maes M, Lin Y-CL, Putarjunan A, Han S-K, Avila J, Torii KU** (2015b)

1111   Competitive binding of antagonistic peptides fine-tunes stomatal patterning. Nature **522**:

1112   439–443

1113   **Lee JS, Kuroha T, Hnilova M, Khatayevich D, Kanaoka MM, Mcabee JM, Sarikaya M,**

1114   **Tamerler C, Torii KU** (2012) Direct interaction of ligand-receptor pairs specifying

1115   stomatal patterning. Genes Dev **26**: 126–136

1116   **Lo HW, Hsu SC, Ali-Seyed M, Gunduz M, Xia W, Wei Y, Bartholomeusz G, Shih JY, Hung**

1117   **MC** (2005) Nuclear interaction of EGFR and STAT3 in the activation of the iNOS/NO

1118   pathway. Cancer Cell **7**: 575–589

1119   **Marti U, Burwen SJ, Wells A, Barker ME, Huling S, Feren AM, Jones AL** (1991)

1120   Localization of epidermal growth factor receptor in hepatocyte nuclei. Hepatology **13**: 15–

1121   20

1122 **Mayer K, Albrecht S, Schaller A** (2015) Targeted analysis of protein phosphorylation by 2D
1123 electrophoresis. Methods Mol Biol **1306**: 167–176

1124 **Miettinen PJ, Berger JE, Meneses J, Phung Y, Pedersen RA, Werb Z, Derynck R** (1995)
1125 Epithelial immaturity and multiorgan failure in mice lacking epidermal growth factor
1126 receptor. Nature **376**: 337–341

1127 **Migliaccio A, Di Domenico M, Castoria G, Nanayakkara M, Lombardi M, De Falco A,**
1128 **Bilancio A, Varricchio L, Ciociola A, Auricchio F** (2005) Steroid receptor regulation of
1129 epidermal growth factor signaling through Src in breast and prostate cancer cells: Steroid
1130 antagonist action. Cancer Res **65**: 10585–10593

1131 **Miller SG, Carnell L, Moore HPH** (1992) Post-Golgi membrane traffic: Brefeldin A inhibits
1132 export from distal Golgi compartments to the cell surface but not recycling. J Cell Biol **118**:
1133 267–283

1134 **Park CJ, Ronald PC** (2012) Cleavage and nuclear localization of the rice XA21 immune
1135 receptor. Nat Commun **3**: 920

1136 **Pastore JJ, Limpuangthip A, Yamaguchi N, Wu MF, Sang Y, Han SK, Malaspina L,**
1137 **Chavdaroff N, Yamaguchi A, Wagner D** (2011) LATE MERISTEM IDENTITY2 acts
1138 together with LEAFY to activate APETALA1. Development **138**: 3189–3198

1139 **Phokas A, Coates JC** (2021) Evolution of DELLA function and signaling in land plants. Evol
1140 Dev **23**: 137–154

1141 **Pignon J-C, Koopmansch B, Nolens G, Delacroix L, Waltregny D, Winkler R** (2009)
1142 Androgen receptor controls EGFR and ERBB2 gene expression at different levels in
1143 prostate cancer cell lines. Cancer Res **69**: 2941–2949

1144 **Plackett ARG, Powers SJ, Fernandez-Garcia N, Urbanova T, Takebayashi Y, Seo M,**
1145 **Jikumaru Y, Benlloch R, Nilsson O, Ruiz-Rivero O, et al** (2012) Analysis of the
1146 Developmental Roles of the Arabidopsis Gibberellin 20-Oxidases Demonstrates That
1147 GA20ox1, -2, and -3 Are the Dominant Paralogs. Plant Cell **24**: 941–960

1148 **Prigent SA, Gullick WJ** (1994) Identification of c-erbB-3 binding sites for phosphatidylinositol
1149 3'-kinase and SHC using an EGF receptor/c-erbB-3 chimera. EMBO J **13**: 2831–2841

1150 **Qi Y, Sun Y, Xu L, Xu Y, Huang H** (2004) ERECTA is required for protection against heat-
1151 stress in the AS1/AS2 pathway to regulate adaxial-abaxial leaf polarity in Arabidopsis.
1152 Planta **219**: 270–276

1153 **Ragni L, Nieminen K, Pacheco-Villalobos D, Sibout R, Schwechheimer C, Hardtke CS**

1154   (2011) Mobile Gibberellin Directly Stimulates Arabidopsis Hypocotyl Xylem Expansion.

1155   Plant Cell **23**: 1322–1336

1156 **Rosa NM la, Pfeiffer A, Hill K, Locascio A, Bhalerao RP, Miskolczi P, Grønlund AL,**

1157   **Wanchoo-Kohli A, Thomas SG, Bennett MJ, et al** (2015) Genome Wide Binding Site

1158   Analysis Reveals Transcriptional Coactivation of Cytokinin-Responsive Genes by DELLA

1159   Proteins. PLOS Genet **11**: e1005337

1160 **Sacharowski SP, Gratkowska DM, Sarnowska EA, Kondrak P, Jancewicz I, Porri A,**

1161   **Bucior E, Rolicka AT, Franzen R, Kowalczyk J, et al** (2015) SWP73 subunits of

1162   arabidopsis SWI/SNF chromatin remodeling complexes play distinct roles in leaf and flower

1163   development. Plant Cell **27**: 1889–1906

1164 **Sáez A, Rodrigues A, Santiago J, Rubio S, Rodriguez PL** (2008) HAB1-SWI3B interaction

1165   reveals a link between abscisic acid signaling and putative SWI/SNF chromatin-remodeling

1166   complexes in Arabidopsis. Plant Cell **20**: 2972–88

1167 **Saleh A, Alvarez-Venegas R, Avramova Z** (2008) An efficient chromatin immunoprecipitation

1168   (ChIP) protocol for studying histone modifications in Arabidopsis plants. Nat Protoc **3**:

1169   1018–1025

1170 **Salem MA, Jüppner J, Bajdzienko K, Giavalisco P** (2016) Protocol: a fast, comprehensive and

1171   reproducible one-step extraction method for the rapid preparation of polar and semi-polar

1172   metabolites, lipids, proteins, starch and cell wall polymers from a single sample. Plant

1173   Methods 2016 121 **12**: 1–15

1174 **Sarnowska E, Gratkowska DM, Sacharowski SP, Cwiek P, Tohge T, Fernie AR, Siedlecki**

1175   **JA, Koncz C, Sarnowski TJ** (2016) The Role of SWI/SNF Chromatin Remodeling

1176   Complexes in Hormone Crosstalk. Trends Plant Sci **21**: 594–608

1177 **Sarnowska EA, Rolicka AT, Bucior E, Cwiek P, Tohge T, Fernie AR, Jikumaru Y, Kamiya**

1178   **Y, Franzen R, Schmelzer E, et al** (2013) DELLA-Interacting SWI3C Core Subunit of

1179   Switch/Sucrose Nonfermenting Chromatin Remodeling Complex Modulates Gibberellin

1180   Responses and Hormonal Cross Talk in Arabidopsis. Plant Physiol **163**: 305–317

1181 **Sarnowski TJ, Swiezewski S, Pawlikowska K, Kaczanowski S, Jerzmanowski A** (2002)

1182   AtSWI3B, an Arabidopsis homolog of SWI3, a core subunit of yeast Swi/Snf chromatin

1183   remodeling complex, interacts with FCA, a regulator of flowering time. Nucleic Acids Res

1184   **30**: 3412–3421

1185   **Schmittgen TD, Livak KJ** (2008) Analyzing real-time PCR data by the comparative CT method.
1186   Nat Protoc **3**: 1101–1108

1187   **Shpak ED** (2003) Dominant-Negative Receptor Uncovers Redundancy in the Arabidopsis
1188   ERECTA Leucine-Rich Repeat Receptor-Like Kinase Signaling Pathway That Regulates
1189   Organ Shape. Plant Cell Online **15**: 1095–1110

1190   **Shpak ED** (2013) Diverse roles of ERECTA family genes in plant development. J Integr Plant
1191   Biol **55**: 1238–1250

1192   **Shpak ED, Berthiaume CT, Hill EJ, Torii KU** (2004) Synergistic interaction of three
1193   ERECTA-family receptor-like kinases controls Arabidopsis organ growth and flower
1194   development by promoting cell proliferation. Development **131**: 1491–1501

1195   **Shpak ED, McAbee JM, Pillitteri LJ, Torii KU** (2005) Stomatal Patterning and Differentiation
1196   by Synergistic Interactions of Receptor Kinases. Science (80-) **309**: 290–293

1197   **Simossis VA, Kleinjung J, Heringa J** (2005) Homology-extended sequence alignment. Nucleic
1198   Acids Res **33**: 816–824

1199   **Stewart M, Turley H, Cook N, Pezzella F, Pillai G, Ogilvie D, Cartlidge S, Paterson D,**
1200   **Copley C, Kendrew J, et al** (2003) The angiogenic receptor KDR is widely distributed in
1201   human tissues and tumours and relocates intracellularly on phosphorylation. An
1202   immunohistochemical study. Histopathology **43**: 33–39

1203   **Tameshige T, Okamoto S, Tasaka M, Torii KU** (2016) Impact of erecta mutation on leaf
1204   serration differs between Arabidopsis accessions. Plant Signal Behav **11 (12)**: 2478–2485

1205   **Torii KU, Mitsukawa N, Oosumi T, Matsuura Y, Yokoyama R, Whittier RF, Komeda Y**
1206   (1996) The Arabidopsis ERECTA gene encodes a putative receptor protein kinase with
1207   extracellular leucine-rich repeats. Plant Cell **8**: 735–746

1208   **Torii KU, Pillitteri LJ, Sloan DB, Bogenschutz NL** (2007) Termination of asymmetric cell
1209   division and differentiation of stomata. Nature **445**: 501–505

1210   **Uchida N, Lee JS, Horst RJ, Lai H-H, Kajita R, Kakimoto T, Tasaka M, Torii KU** (2012a)
1211   Regulation of inflorescence architecture by intertissue layer ligand-receptor communication
1212   between endodermis and phloem. Proc Natl Acad Sci **109**: 6337–6342

1213   **Uchida N, Shimada M, Tasaka M** (2013) ERECTA-family receptor kinases regulate stem cell
1214   homeostasis via buffering its cytokinin responsiveness in the shoot apical meristem. Plant

1215   Cell Physiol **54**: 343–351

1216   **Uchida N, Shimada M, Tasaka M** (2012b) Modulation of the balance between stem cell

1217   proliferation and consumption by ERECTA-family genes. Plant Signal Behav **7**: 1506–1508

1218   **Willige BC, Ghosh S, Nill C, Zourelidou M, Dohmann EMN, Maier A, Schwechheimer C**

1219   (2007) The DELLA domain of GA INSENSITIVE mediates the interaction with the GA

1220   INSENSITIVE DWARF1A gibberellin receptor of Arabidopsis. Plant Cell **19**: 1209–1220

1221   **Wojtyla Ł, Rucińska-Sobkowiak R, Kubala S, Garnczarska M** (2013) Lupine embryo axes

1222   under salinity stress. I. Ultrastructural response. Acta Physiol Plant **35**: 2219–2228

1223   **Wong RWC** (2003) Transgenic and knock-out mice for deciphering the roles of EGFR ligands.

1224   Cell Mol Life Sci **60**: 113–118

1225   **Woodward AW, Bartel B** (2005) A receptor for auxin. Plant Cell **17**: 2425–2429

1226   **Yarden Y, Sliwkowski MX** (2001) Untangling the ErbB signalling network. Nat Rev Mol Cell

1227   Biol **2**: 127–137

1228   **Van Zanten M, Basten Snoek L, Van Eck-Stouten E, Proveniers MCG, Torii KU, Voesenek**

1229   **LACJ, Peeters AJM, Millenaar FF** (2010) Ethylene-induced hyponastic growth in

1230   Arabidopsis thaliana is controlled by ERECTA. Plant J **61**: 83–95

1231   **Zentella R, Zhang Z-L, Park M, Thomas SG, Endo A, Murase K, Fleet CM, Jikumaru Y,**

1232   **Nambara E, Kamiya Y, et al** (2007) Global analysis of della direct targets in early

1233   gibberellin signaling in Arabidopsis. Plant Cell **19**: 3037–3057

1234   **Zhang L, DeGennaro D, Lin G, Chai J, Shpak ED** (2021) ERECTA family signaling

1235   constrains CLAVATA3 and WUSCHEL to the center of the shoot apical meristem.

1236   Development. doi: 10.1242/DEV.189753

1237